

Structural complementarity and similarity: linking relational principles to network motifs

Szymon Talaga^{1*}

Andrzej Nowak^{2,3}

¹Robert Zajonc Institute for Social Studies, University of Warsaw,
Stawki 5/7, 00-183 Warsaw, Poland.

²Faculty of Psychology, University of Warsaw,
Stawki 5/7, 00-183 Warsaw, Poland.

³Department of Psychology, Florida Atlantic University,
777 Glades Rd, Boca Raton, FL 33431, USA.

*Corresponding author; E-mail: stalaga@uw.edu.pl

Abstract

The principle of similarity, or homophily, is often used to explain prevalent patterns observed in complex networks such as transitivity and abundance of triangles (3-cycles). On the other hand, many phenomena, from division of labor to protein-protein interactions (PPI), are driven by complementarity, or differences and synergy. However, the principle of complementarity has not been operationalized in network terms. Here we show that complementarity is linked to the abundance of quadrangles (4-cycles) and the presence of dense bipartite-like subgraphs. Starting from simple geometric arguments we link similarity and complementarity to their characteristic network motifs and introduce two families of coefficients: (1) structural similarity generalizing the notions of local clustering and closure and capturing the full spectrum of similarity-driven structures; (2) analogous complementarity coefficients based on quadrangles instead of triangles. We demonstrate on a variety of social and biological networks that the coefficients capture important structural properties which can be related to meaningful domain-specific phenomena. We show that they can be used to distinguish between different kinds of social relations and measure an increasing structural diversity of PPI networks across the tree of life. Our results suggest that for some types of relations assuming homophily may not be adequate. Moreover, they can be used to inform link prediction methods and decide when assuming triadic or tetradic closure is more appropriate. More generally, we provide a novel set of tools for studying the structure of networks in terms of complementarity between their elements. We also provide an efficient Python implementation of the proposed methods.

Keywords— similarity | complementarity | complex networks | network motifs | network geometry

1. Introduction

The structure of complex networks commonly reflects their functional properties as well as mechanisms or processes that created them. Seminal studies have shown that different systems, from neural networks to the World Wide Web, tend to be characterized by the presence of statistically over-represented small subgraphs, known as network motifs [48, 58, 64]. While it is natural to expect different motifs to be related to particular functions or properties of a given system, it is often not easy to determine what they are exactly. In some cases and specific contexts, such as gene regulatory networks, the roles played by different motifs may be revealed through experimental studies [3, 58]. However, general principles that would explain the prevalence of specific motifs across different domains are still mostly unknown.

An important exception is the widely-known abundance of triangles (3-cycles) in many types of real-world networks, which has been shown to be a structural signature of transitive relations driven by similarity between nodes in some (possibly latent) metric space [11, 12, 36]. The importance of similarity and its impact on the

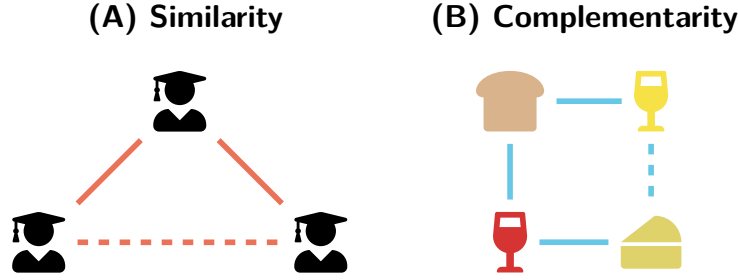


Figure 1. Intuitive meaning of similarity and complementarity. **(A)** If three persons are similar (e.g. they are all scientists) and we know that one of them (top) knows the two others (bottom) it is quite likely that they know each other too (dashed line). Thus, the relation is **transitive**. **(B)** If one wine (red) goes well with (is complementary to) bread and cheese and another wine (white) also goes well with the bread, then it is likely that it is a good match for the cheese too (dashed line). However, this does not imply that both wines will be drunk together, so the relation is **not transitive**.

structure of social networks has been recognized in sociology for a long time, as it is linked to homophily and triadic closure [6, 34, 42, 47, 62]. While it is usually hard to disentangle their effects [4, 5], these two processes are also inherently linked as they lead to structural similarity between connected nodes. In other words, in similarity-driven systems two adjacent nodes are likely to share a lot of neighbors (Fig. 1A), and this implies the abundance of triangles and a latent geometric structure [36, 51].

Geometry induced by similarity has been often used for defining statistical models of social networks [30, 37], as well as networks from other domains, including protein-protein interaction and brain networks [2, 29] or the Internet [13]. Moreover, geometric representations of social systems have a long tradition in sociology [10, 14, 46].

In this light, it is natural to ask whether there are other general relational principles akin to similarity that are linked to their characteristic network motifs, possibly thanks to some kind of an intrinsic geometry? Here we show that one such principle is complementarity, which organizes relations driven by differences and synergies and is linked to the abundance of quadrangles (4-cycles) and the presence of locally dense bipartite-like subgraphs.

Indeed, many important phenomena, from cooperation, business interactions and division of labor [16, 21, 27, 44, 55, 70] to the quality of romantic relationships [41], consumer choices [63] and at least some types of protein-protein binding [35], may be better explained by complementarities, or differences and synergies, between diverse features of the involved parties. For instance, two types of wine may be often bought together with the same kinds of bread and cheese but rarely both of them will occur in the same transaction. In other words, in this situation a wine is complementary to the bread and cheese, but not to the other wine (Fig. 1B). More generally, complementarity can be seen as a particular interpretation of the principle of heterophily, which is a preference for connecting to others who are different with respect to some salient attributes [55]. Crucially, as we show later, the principle of complementarity, unlike the general notion of heterophily, has a natural geometric interpretation which links it to quadrangles as its characteristic motif.

In order to formalize our analysis, we first define a fully general family of similarity coefficients measuring the abundance of triangles at the levels of individual nodes and edges as well as entire graphs. The coefficients generalize the notions of local clustering and closure [68, 71] and therefore capture the full spectrum of transitive, similarity-driven structures. Then, starting from a simple geometric model of complementarity we follow the same logic as in the case of similarity and define an analogous family of complementarity coefficients measuring the abundance of quadrangles.

We will call the proposed measures *structural coefficients* because they will not be defined with respect to node attributes, latent or observed, but to how different nodes are embedded in the network. Moreover, we will show that they are closely linked to the fundamental notions of transitivity and structural equivalence [49, 67].

We study the behavior of structural coefficients in some of the most important random graph models as well as multiple real-world social and biological networks. We demonstrate that they are related to meaningful domain-

specific phenomena and can be used to distinguish between different types of networks. In particular, we show that they discriminate effectively between different kinds of social relations and may be used to measure the increasing structural diversity of protein-protein interaction (PPI) networks, or interactomes, across the tree of life.

Our results complement the rich literature on network motifs and network geometry as well as provide a principled theory and methods linking different types of relations to their observable structural signatures. Our work also shows that the customary assumption of homophily is not adequate for some types of social relations and provides principled tools for identifying such systems, bringing more nuance to the field of social network analysis. Moreover, the framework we propose could be, in principle, used for improving current link prediction methods by helping to determine when the assumption of 2-path (L2) or 3-path (L3) closure [35] is more appropriate.

Last but not least, all methods introduced in this paper are implemented in a Python package called **pathcensus** (see Materials and Methods).

Notation & technical remarks

In this paper we consider simple undirected and unweighted graphs $G = (V, E)$. We use $n = |V|$ and $m = |E|$ to denote the numbers of nodes and edges in G respectively. Elements of the adjacency matrix of a graph G will be denoted by a_{ij} and assumed to be equal to 1 if the edge (i, j) exists and 0 otherwise. For any node $i \in V$ we denote its degree by d_i and its k -hop neighborhood by $\mathcal{N}_k(i)$, in particular 1-hop neighborhood will be denoted by $\mathcal{N}_1(i)$. Moreover, we will use $n_{ij} = |\mathcal{N}_1(i) \cap \mathcal{N}_1(j)|$ to denote the number of shared neighbors between nodes i and j . Averaged quantities will be denoted by diamond brackets. For instance, $\langle d_i \rangle$ will denote average node degree.

2. Results

2.1. Structural similarity

It is natural to think about similarity in terms of distance between different objects in a feature space. Hence, the motivating geometric model for similarity-driven relations posits that nodes are positioned in some metric space and the probability of observing a link between them is a decreasing function of the corresponding distance. Such a generic model can be seen as an instance of the class of Random Geometric Graphs (RGG) [12, 62]. The crux is that this very general formulation is enough to guarantee the abundance of triangles (3-cycles) (see Fig. 2A).

Hence, a natural starting point for our endeavor is *local clustering coefficient* [68], of which value for a node i will be denoted by s_i^W . It is a classical network measure of the density of the 1-hop neighborhood (ego-network) of i and it is defined as:

$$s_i^W = \frac{2T_i}{t_i^W} \quad (1)$$

where T_i is the number of triangles including i and t_i^W is the number of wedge triples centered at i or 2-paths with i in the middle (Fig. 2B). Crucially, $s_i^W \in [0, 1]$ and is equal to 1 if and only if $\mathcal{N}_1(i)$ forms a fully connected network. In sociological terms, it measures the extent to which *my friends are friends with each other*. Note, however, that this is only one side of the triadic closure process as it corresponds to the closing of the loop between friends of the focal node i . The other part is about the loop between i and friends of its friends and local clustering coefficient does not capture it.

To address this issue an alternative *local closure coefficient* [71] has been proposed more recently:

$$s_i^H = \frac{2T_i}{t_i^H} \quad (2)$$

where t_i^H is the number of head triples originating from i , that is, 2-paths starting at i (Fig. 2C). It is also in the range of $[0, 1]$ and attains the maximum value if and only if no neighbor of i is adjacent to a node which is not already in $\mathcal{N}_1(i)$. In other words, when $s_i^H = 1$ a random walker starting at i will never leave $\mathcal{N}_1(i)$. Thus, local closure coefficient measures the extent to which *friends of my friends are my friends*, that is, it is a measure of triadic closure between the focal node i and neighbors of its neighbors. As a result, it captures exactly that what

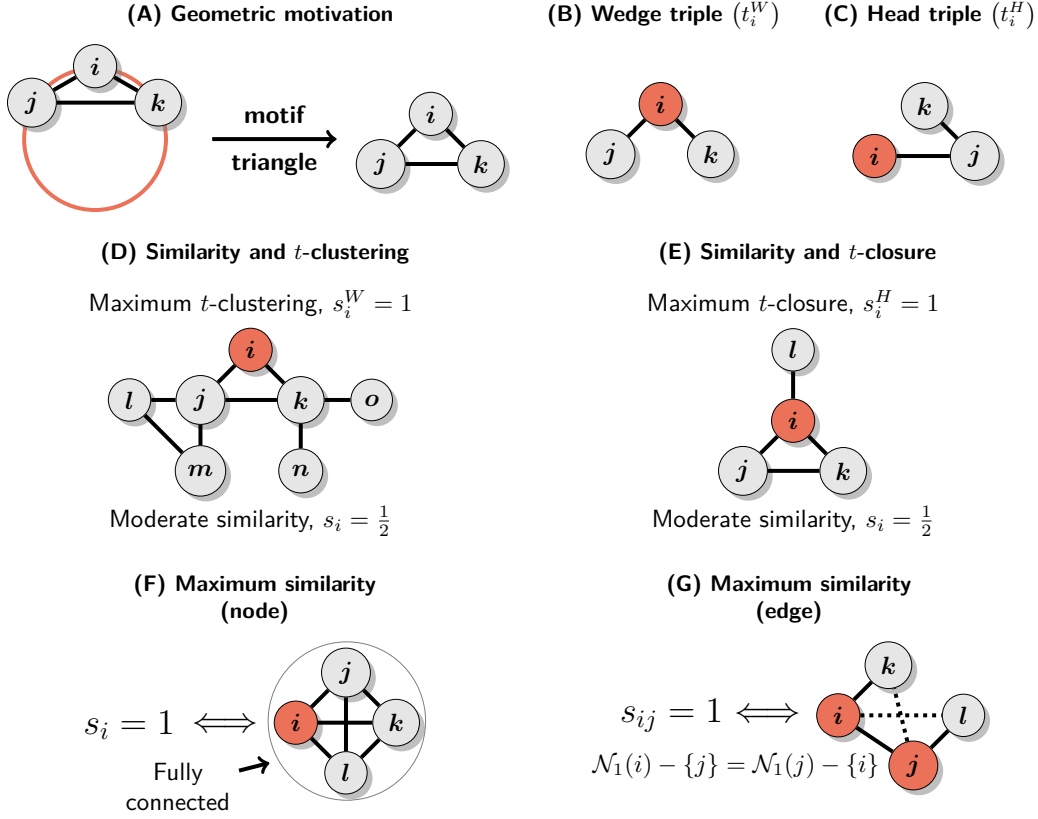


Figure 2. Geometric motivation and the main properties of structural similarity coefficients. (A) Metric structure induced by similarity implies transitivity of relations and the abundance of triangles. (B and C) Wedge and head triples. (D) Local clustering can be maximized even when neighbors of the focal node are very differently embedded within the network, while s_i is sensitive to this kind of non-transitivity. (E) Local closure can be maximized even for nodes with sparse 1-hop neighborhoods if they are star-like as neighbors with degree one do not generate any head triples. On the other hand, s_i is sensitive to this kind of non-transitivity. (F and G) Necessary and sufficient conditions for maximum structural similarity coefficient at the levels of nodes and edges.

local clustering is blind to. Since the local clustering and closure coefficients are based on triples we will later refer to them as t -clustering and t -closure respectively.

The two coefficients complement each other, so it is only natural to combine them in a single measure. We now propose such a measure which we will call *structural similarity coefficient*:

$$s_i = \frac{4T_i}{t_i^W + t_i^H} = \frac{t_i^W s_i^W + t_i^H s_i^H}{t_i^W + t_i^H} \quad (3)$$

Note that s_i is equal to the fraction of both wedge and head triples including i which can be closed to make a triangle. It is also equivalent to a weighted average of s_i^W and s_i^H , which implies that $\min(s_i^W, s_i^H) \leq s_i \leq \max(s_i^W, s_i^H)$. Moreover, since $s_i^W = 1$ if and only if $\mathcal{N}_1(i)$ is fully connected and $s_i^H = 1$ if there are no links leaving $\mathcal{N}_1(i)$ then it must be that $s_i = 1$ if and only if i belongs to a fully connected network. Fig. 2 provides a summary of the motivation and main properties of s_i , including examples of when t -clustering and t -closure coefficients are maximal while structural similarity is only moderate (Figs. 2D and 2E).

Crucially, unlike local clustering and closure, structural similarity coefficient captures the full spectrum of local structures implied by the transitivity of similarity-driven relations.

2.1.1. Edge-wise similarity and structural equivalence

Structural similarity can also be defined for edges. In this case it is equal to the ratio of triangles including nodes i and j to the total number of 2-paths traversing the (i, j) edge (Fig. 2G). In other words, it is equivalent to the number of shared neighbors relative to the total number of neighbors of i and j , excluding i and j themselves:

$$s_{ij} = \frac{2T_{ij}}{t_{ij}^W + t_{ij}^H} = \frac{2n_{ij}}{d_i + d_j - 2} \quad (4)$$

where T_{ij} is the number of triangles including i and j , t_{ij}^W is the number of (k, i, j) and t_{ij}^H of (i, j, k) triples. Importantly, s_{ij} is symmetric since $T_{ij} = T_{ji}$ and $t_{ij}^W = t_{ji}^H$.

Note that s_{ij} is closely related to the Sørensen Index or normalized Hamming similarity [49, 60], $H_{ij} = 2n_{ij}/(d_i + d_j)$, and differs only in the -2 term in the denominator which accounts for the fact that i and j are known to be connected. Hamming distance/similarity is one of the common measures of structural equivalence [Sec. 7.12.3 in 49] which implies that the proposed node-wise similarity coefficient can be seen as a proxy for the extent to which i is structurally equivalent to its own neighbors. We elaborate on this and formally derive the connection to structural equivalence in the Supplementary Information (SI: S1).

2.1.2. Global similarity

From the global perspective both local clustering and local closure lead to the same conclusion that the corresponding global measure is just the fraction of triples that can be closed to make a triangle [71]. This implies that the same quantity is also the proper global measure of the extent to which relations are driven by similarity. In other words, the *global similarity coefficient* is equal to the standard global clustering coefficient and can be defined as:

$$s = \frac{3T}{\sum_i d_i(d_i - 1)} \quad (5)$$

where T is the total number of triangles and the denominator counts the number of triples.

Note that it is indeed a reasonable measure of similarity-driven relations as it is maximized only when a network is fully connected, so all nodes are structurally redundant and can be removed without affecting the overall connectivity.

2.2. Structural complementarity

First, let us consider an intuitive meaning of complementarity. We posit that two objects are complementary when their features are different but in a well-defined synergistic way. As we will see, this additional synergy constraint is crucial. However, before we discuss this further let us note that in the case of similarity an analogous constraint is built-in by design. It is so, because for any point there is always only one point minimizing the distance in the feature space (maximizing similarity) and it is the point itself. Hence, it is arguably natural to say that any object is most similar to itself. As a result, there is a well-defined notion of maximal similarity.

On the other hand, the case of difference is more complex. To make our argument more concrete, let the feature space be \mathbb{R}^k with $k \geq 1$. Now, it is easy to see that for any two points p and r at a distance $d(p, r)$ we can find a third point s such that $d(p, s) > d(p, r)$. In other words, for any point p there is no well-defined point at the maximum distance. Thus, complementarity cannot be defined in terms of arbitrary differences. Intuitively, defining it in terms of a simple unconstrained heterophily inevitably leads to the conclusion that for any object there is an infinite variety of more and more complementary (different) objects, which clearly does not map well on the common understanding of the notion of complementarity. Thus, we need a definition with the same property as in the case of similarity, that is, one yielding a sequence of ever smaller sets of more and more complementary elements converging to a single well-defined point in the limit of maximum complementarity.

Note that the above abstract argument can be related to known complementarity-driven systems in a rather straightforward manner. For instance, a key and a lock are complementary not because they are just different in an arbitrary fashion, but because they differ in a very specific way by being structural negatives of each other. Similarly,

division of labor in modern societies is based on complex synergies between capabilities of different individuals and organizations.

Thus, we argue that complementarity should be defined in terms of distance maximization but with additional constraints ensuring that for any point in the feature space there is only one point at the maximum distance. This can be achieved in several ways, but to keep things simple we will focus on one particularly natural and convenient solution.

We consider nodes as placed on the surface of a k -dimensional (hyper)sphere with $k \geq 1$. In this setting for each point there is only a single point at the maximum distance and the maximum distance is the same for all points. Now, if nodes connect preferentially to others who are far away, we obtain a model analogous to similarity, but now the connections of a node are not concentrated in its vicinity but instead on the other side of the space. From this it follows that any two connected nodes i and j will not share a lot of neighbors, so triangles will be rare, but instead the 1-hop neighborhood of i should be approximately equal to the 2-hop neighborhood of j and *vice versa*, that is, $\mathcal{N}_1(i) \approx \mathcal{N}_2(j)$ and $\mathcal{N}_2(i) \approx \mathcal{N}_1(j)$. Such a spatial structure inevitably leads to the abundance of quadrangles (4-cycles) and in general locally dense bipartite-like subgraphs (Fig. 3A).

Note that the choice of a (hyper)sphere surface is far from arbitrary as it is a specific instance in the broader class of compact homogeneous and isotropic manifolds, for which it has been shown that it is a proper choice for a latent geometry capable of reproducing jointly sparsity with high clustering, small-world effect and arbitrary degree distributions in similarity-driven networks [12]. In other words, in this setting latent geometry can explain some of the most fundamental structural properties of many real-world networks, in particular social networks [62]. Thus, we argue, it is also a natural first choice for representing relations driven by complementarity, especially that thanks to its structure it seems particularly well-suited for this task (but see Ref. [33] for an alternative approach).

Depending on the context different authors may refer to slightly different objects when using the term *quadrangle*. Namely, a quadrangle may contain up to two chords or diagonal links between its vertices. Here we will consider only quadrangles without any chords, which we will call *strong quadrangles*. This choice follows, of course, from the proposed geometric model and the fact that only strong quadrangles are characteristic for locally dense bipartite-like graphs.

Now we can start defining coefficients measuring relations driven by complementarity. As previously, we begin with a local clustering coefficient, which will be called q -clustering. It is defined analogously, but this time in terms of quadrangles and wedge quadruples, that is, 3-paths with the focal node i at the second position (Fig. 3B):

$$c_i^W = \frac{2Q_i}{q_i^W} \quad (6)$$

where Q_i is the number of strong quadrangles incident to the focal node i and q_i^W is the number of wedge quadruples it belongs to. Note that we consider only quadruples with i at the second position, such as (l, i, j, k) but not (k, j, i, l) , in order to avoid double counting and make the number of wedge and head quadruples per quadrangle equal. Intuitively, it quantifies the extent to which the local environment of i is bipartite-like and its neighbors are structurally equivalent to each other.

Local q -closure coefficient is defined in the same way as the fraction of head quadruples originating from i (Fig. 3C) that can be closed to make a (strong) quadrangle:

$$c_i^H = \frac{2Q_i}{q_i^H} \quad (7)$$

where q_i^H is the number of head quadruples starting at i . Conceptually, it measures the extent to which the local environment of i is bipartite-like and i is structurally equivalent to its 2-hop neighbors.

We can now define *structural complementarity coefficient* as the fraction of quadruples including the focal node i which can be closed to make a (strong) quadrangle which, again, is equivalent to a weighted average of q -clustering and q -closure:

$$c_i = \frac{4Q_i}{q_i^W + q_i^H} = \frac{q_i^W c_i^W + q_i^H c_i^H}{q_i^W + q_i^H} \quad (8)$$

Note that again we have that $\min(c_i^W, c_i^H) \leq c_i \leq \max(c_i^W, c_i^H)$, so c_i is always bounded between its constitutive clustering and closure coefficients. Moreover, the interpretations of q -clustering and q -closure jointly imply that

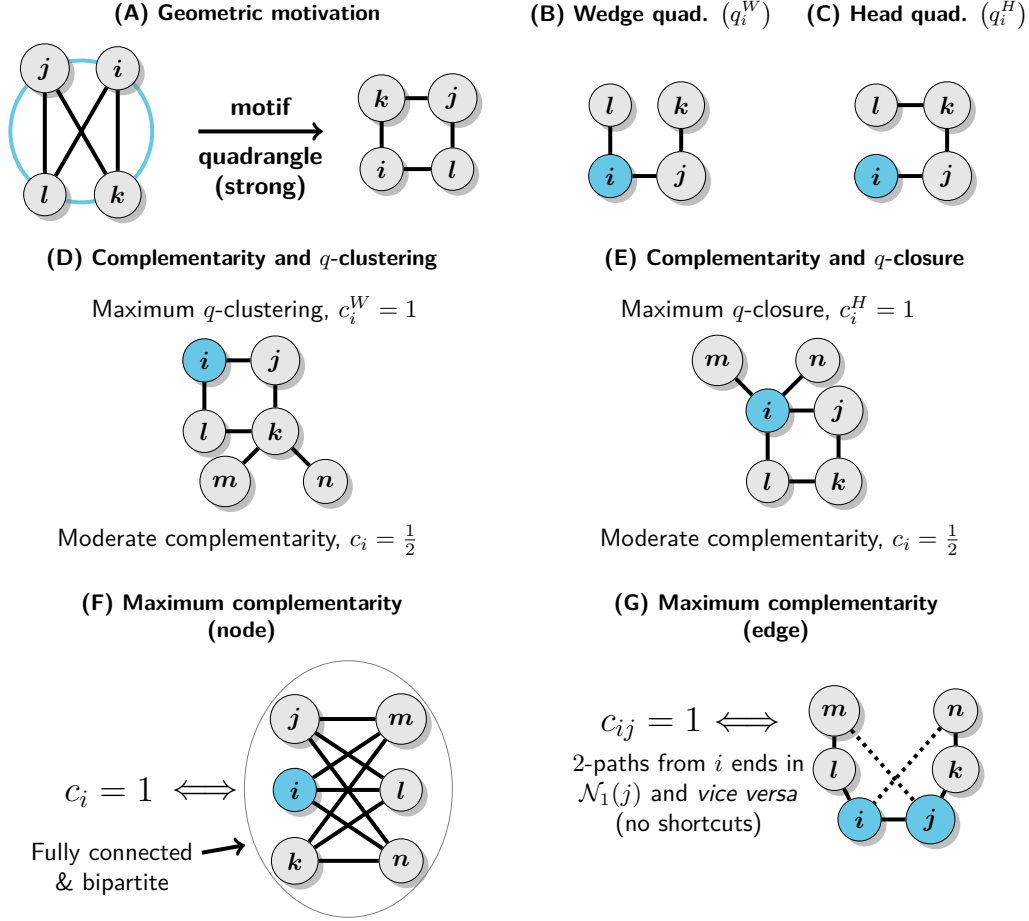


Figure 3. Geometric motivation and the main properties of structural complementarity coefficients. (A) On the surface of a (hyper)sphere for each point there is only a single other point at the maximum distance, so complementarity based on distance maximization must lead to the abundance of strong (chordless) quadrangles and locally dense bipartite-like subgraphs. More generally, the geometry of complementarity induces non-transitive relations, which are still localized and non-random in the sense that if two nodes share one neighbor then they are probably not directly connected but share also other neighbors, so instead they are structurally equivalent. This leads to quadrangle closure. (B and C) Wedge and head quadruples. (D) Local q -clustering can be maximized even when some 2-hop neighbors (node k on the figure) of the focal node connect to nodes which are not in $\mathcal{N}_1(i)$, while the c_i is sensitive to this deviation from the principle of complementarity. (E) Local q -closure can be maximized even for nodes with sparse 1-hop neighborhoods if they are star-like as neighbors with degree one do not generate any head quadruples. (F and G) Necessary and sufficient conditions for maximum structural complementarity coefficient at the levels of nodes and edges.

$c_i = 1$ if and only if the focal node i belongs to a fully connected bipartite network. Fig. 3 presents a summary of the most important terms and facts related to c_i .

The geometric model underlying the definition of c_i indeed justifies the interpretation in terms of complementarity or synergy. Nodes are more likely to be connected when they are far away in the feature space, meaning that they have different properties which can be possibly combined in a synergistic manner. Crucially, the mesoscopic network structure that is implied by this model is also related to complementarity in a straightforward manner. Bipartite networks are representations of complementarity-driven systems *par excellence* as they consist of two types of nodes and allow only for connections between them. Hence, c_i , being a combined measure of local bipartiteness and density, is actually indicative of the degree to which the local environment of a node resembles such a complementarity-driven system. Note that the fact that c_i is constrained by the density of bipartite connections is crucial as tree-like networks are also locally bipartite-like (i.e. $\mathcal{N}_1(i)$ corresponds to the first type and $\{i\} \cup \mathcal{N}_2(i)$ to

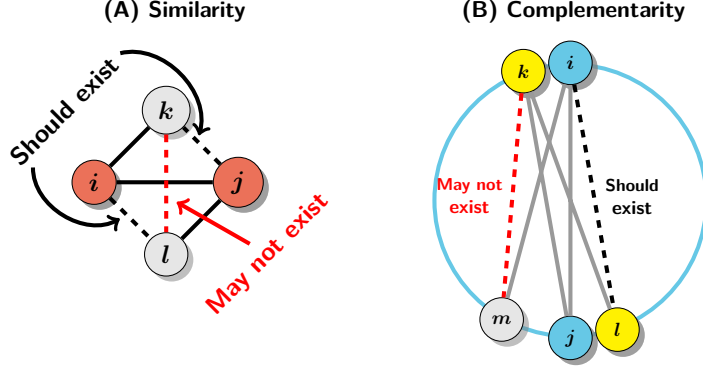


Figure 4. Interpretation of the edge-wise structural coefficients. **(A)** If (i, j) edge is driven by similarity then any neighbor of either i or j (k and l on the figure) should be near i (or j) in the latent space making it likely that it links to the other member of the (i, j) pair too. On the other hand, k and l may still be quite far away so the link between them may not exist. **(B)** If (i, j) edge is driven by complementarity then any 2-hop neighbor of j (i), such as l (k) on the figure, should be a 1-hop neighbor of i (j). The quadruple (i, j, k, l) on the figure corresponds to such a situation. On the other hand, any pair of neighbors of i and j correspondingly may be located in the latent space close enough to each other as to make a tie between them unlikely (as it happens for nodes m and k on the figure).

the second) but in a trivial way as connections between the two “types” of nodes are very sparse, indicating rather a random organization, or at least such a structure cannot be interpreted as compelling evidence of complementarity.

Note that our measures of structural complementarity are based on strong (chordless) quadrangles and hence are different from alternatives such as those proposed in Ref. [31], where authors used a weak definition of quadrangles allowing for any number of chords. This is important as only strong quadrangles lead to definitions which can be interpreted strictly in terms of dense locally bipartite structures and this, as we argue, is crucial for measuring complementarity-driven relations.

Furthermore, when applied to purely bipartite networks the quadrangle-based measures can be seen as a generalization of the bipartite clustering coefficient(s) [50, 73]. However, the crux is that our quadrangle-based complementarity coefficients can be applied to unipartite networks in order to quantify jointly local bipartiteness and density, which together are indicative of complementarity-driven relations.

2.2.1. Edge-wise complementarity and structural equivalence

Structural complementarity may be measured also at the level of edges (Fig. 3G). The edge-wise coefficient is defined as:

$$c_{ij} = \frac{2Q_{ij}}{q_{ij}^W + q_{ij}^H} \quad (9)$$

where Q_{ij} is the number of quadrangles including nodes i and j , q_{ij}^W is the number of (j, i, k, l) and q_{ij}^H of (i, j, k, l) quadruples. Again, $Q_{ij} = Q_{ji}$ and $q_{ij}^W = q_{ji}^H$ so c_{ij} is symmetric.

This way c_{ij} can be seen as a joint measure of bipartiteness around an (i, j) edge and structural equivalence between i and 1-hop neighbors of j and *vice versa*. It measures the extent to which $N_2(i) \approx N_1(j)$ and $N_1(i) \approx N_2(j)$ without requiring dense connections between the 1-hop and 2-hop neighborhoods of i and j . Note that this is analogous to edge-wise similarity which measures only the extent to which $N_1(i) \approx N_1(j)$ without considering the density of connections between the neighbors of i and j as this would be a higher-order property unrelated to whether an edge is driven by similarity or not (see Fig. 4 for details). We derive and discuss in detail the connection to structural equivalence in the SI: S2.

2.2.2. Global complementarity coefficient

From the global perspective of an entire network there is of course no difference between wedge and head quadruples. Hence, the global coefficient can be defined simply as:

$$c = \frac{4Q}{\sum_{i,j} (d_i - 1)(d_j - 1) - n_{ij}} \quad (10)$$

where $(i, j) \in E$ and Q is the total number of quadrangles with no chords. The denominator counts the total number of quadruples. Note that $c = 1$ if and only if the graph as such is fully connected and bipartite. This agrees with the intuition as this is exactly the structure one should expect in a system composed of two classes of elements in which each element in one class is perfectly complementary to every element in the other.

2.3. Structural coefficients in random graphs

We discuss the behavior of structural coefficients in some of the most important random graph models as such results can be used as natural benchmarks against which to compare and calibrate values observed in real-world networks.

2.3.1. Erdős–Rényi model

In the Erdős–Rényi (ER) model [22] the expected global similarity, which is of course equivalent to global clustering, is simply $\mathbb{E}[s] = p$, or equal to the probability that any edge exists. This is a standard result that follows from the fact that for any (i, j, k) triple the closing (i, k) edge always exists with probability p [Sec. 12.4 in 49].

We can use a similar argument to derive the expected value of global complementarity coefficient in the ER model. Let (i, j, k, l) be any connected quadruple. It forms a quadrangle with no chords if and only if the (i, l) edge exists while the (i, k) and (j, l) edges do not. Since all edges in the ER model exist independently with probability p it means that the expected value of global complementarity coefficient is $\mathbb{E}[c] = p(1 - p)^2$.

2.3.2. Configuration model

A natural null model for studying node-wise coefficients and their correlations with node degrees is the configuration model in which a particular degree sequence is enforced while apart from that connections are established as randomly as possible [cf. Sec. 13.2 in 49]. In order to describe the qualitative behavior of the node-wise structural similarity and complementarity we will use the fact that in both cases they are bounded by their corresponding clustering and closure coefficients.

First, note that it is usually conjectured that t -clustering should generally decrease with node degree [Sec. 8.6.1 in 49]. More recently, it was analytically proven for the family of random networks with power law degree distributions that t -clustering is on average roughly constant for low-degree nodes and then starts to decrease more quickly as node degree grows [66].

On the other hand, it has been shown that local closure coefficient, or t -closure in our terminology, is positively correlated with node degree in the configuration model [71]. Thus, these two results together imply that structural similarity s_i can display rich, also non-monotonic, correlations with node degrees depending on the structure of a particular network.

We leave analytical study of the analogous properties of q -clustering and q -closure for future work. However, since both types of clustering and closure coefficients are based on either wedge or head triples/quadruples and therefore are very similar by construction, we conjecture that they should display the same qualitative behavior in the configuration model. Namely, we expect that q -clustering should decrease with node degree, especially for well-connected nodes, and q -closure should increase with node degree. As a result, we also expect that structural complementarity should vary with respect to node degree in various, also non-monotonic, ways.

Indeed, our theoretical expectations agree with average trends observed in randomized networks sampled from Undirected Binary Configuration Model (UBCM) [65] fitted to degree sequences of 28 real-world networks. See the SI: S4 and Fig. S1 for details. An important practical implication is that structural coefficients depend on node

degrees even in random graphs and therefore when comparing different networks their values should be calibrated based on a plausible null model such as UBCM to account for the effects induced purely by the first-order structure (degree sequences).

2.4. Structural coefficients in real networks

We studied structural similarity and complementarity in multiple real-world social and biological networks measuring different kinds of relations — friendship, trust and recognition for social networks as well as gene transcription regulation and general protein-protein interactions (interactomes) for biological networks (see Fig. 5 for details). The goal was to see whether structural similarity and complementarity can be related to some meaningful domain-specific properties of different types of networks.

Our results show that similarity and complementarity in social networks are indeed related to different types of relations. In particular, similarity is stronger in systems driven by homophily or what can be called self-preference, that is, preference for connecting to others who are similar to us, which naturally leads to the transitivity of relations. The importance of similarity seems to be particularly strong for relations depending on close ties such as friendship or trust. This is consistent with decades of research on social networks [34, 42, 47, 54]. On the other hand, it seems that complementarity plays an important role in shaping of relations in which preferences are decoupled from the properties of the ego, such as recognition (e.g. of value or importance of others), skill-based collaboration [70] or trade/business interactions [44]. In this case two agents with similar preferences should typically connect to the same neighbors (and therefore be structurally equivalent) but not necessarily to each other, as the preferences of an agent do not have to match its intrinsic properties. This leads naturally to the abundance of quadrangles and the presence of locally dense bipartite-like subgraphs, that is, the structural signatures of complementarity. Interestingly, even though such preference-based relations are not directly transitive, they can be considered second-order transitive due to the implied mechanism of quadrangle closure (see Fig. 5B). We put this tentative hypothesis to a more direct and systematic test in the next section.

Most of the biological networks feature both relatively high similarity and complementarity. This is consistent with multiple results concerning network motifs characteristic for interactomes as well as neural and gene transcription regulatory networks [48, 58, 64]. Namely, structural similarity is linked to the presence of feed-back and feed-forward loops which, when edge directions are unknown or ignored, explains the abundance of triangles. On the other hand, structural complementarity is connected to motifs such as bi-fan and bi-parallel [48], which imply the abundance of quadrangles (see Fig. 5D). Importantly, these structural patterns can be linked to meaningful domain-specific complementarities between different subsets of elements of a system. For instance, in gene transcription regulatory networks bipartite-like subgraphs with high density of bi-fan motifs (quadrangles) represent dense overlapping regulons (DOR) or groups of operons regulated by similar combinations of input transcription factors [58].

Our results also point to important differences between social and biological networks. The former, with some exceptions of course, tend to be dominated by similarity while the latter are more structurally diverse, which probably reflects their heterogeneous functional properties and complex evolutionary history. This is consistent with observations of a gradual shift from the domination of triangles to an increasing abundance of quadrangles in protein neighborhoods during evolution [74]. However, it seems that large online social networks also feature increased complementarity relatively often (see Fig. 5A). Thus, it may be worthwhile to study differences between small and large as well as offline and online social networks in the future. In particular, to our best knowledge it is not yet clear what social processes are responsible for significantly high amounts of quadrangles in large online social networks.

2.5. Similarity and complementarity in social relations

Here we test the hypothesis that social relations based on homophily, or self-preference, are linked to structural similarity and those based on preference, recognition and skill-based collaboration to structural complementarity. For this purpose, we used a set of 34 social networks collected in 17 rural villages in Mayuge District, Uganda [15]. For each village two networks of relations between households were measured: (1) a friendship network and (2) a health advice network (see Materials and Methods for details).

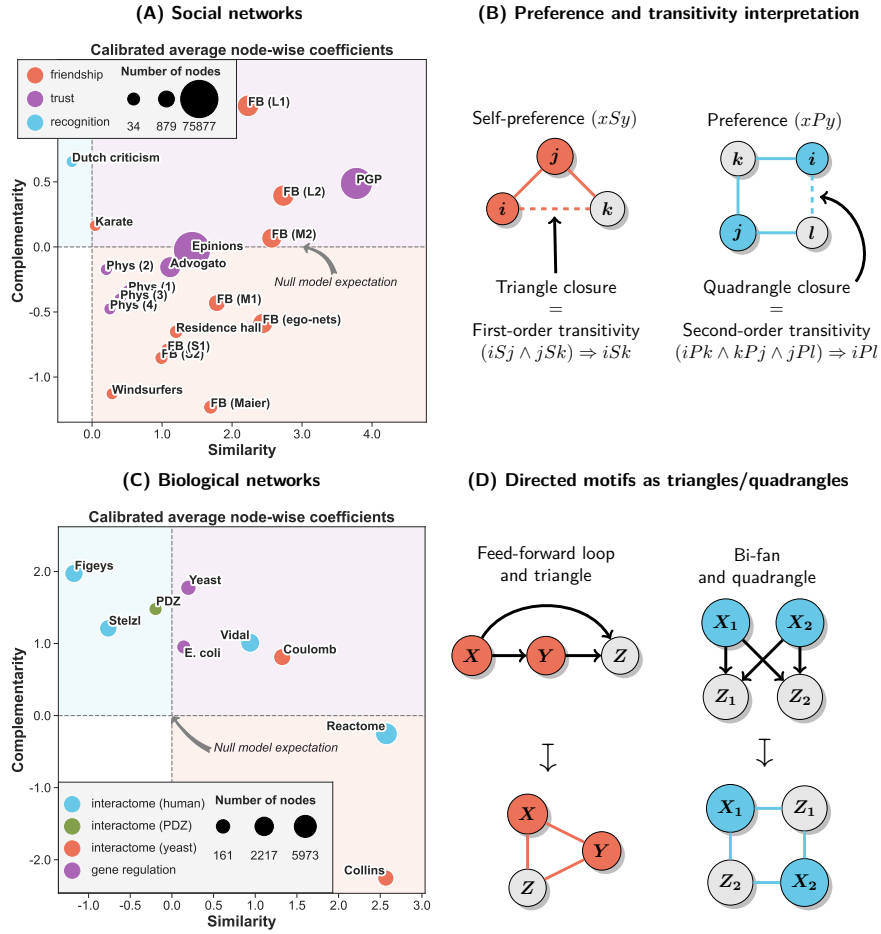


Figure 5. Structural similarity and complementarity in different kinds of social (19 cases) and biological (9 cases) networks (see Materials and Methods for details). Scatterplots show calibrated average node-wise coefficients (see the SI: S5) with dashed lines indicating null model expectations based on UBCM. Quadrants of the plots are colored to indicate different configurations of increased values of similarity and complementarity coefficients — high and low (red), low and high (blue), both high (violet). **(A)** Social networks. Almost all networks feature high structural similarity and some of them also increased complementarity (these are mostly large online social networks). The only case with low similarity and relatively high complementarity is the network of Dutch literary criticism representing relationships of recognition (mentioning other’s work, positively or negatively, in an essay or an interview) within a set of notable literary authors [20]. Its high structural complementarity indicates a relative abundance of quadrangles as the characteristic motif within the network. This reflects the non-transitive, preference-based character of the relation of recognition. **(B)** Interpretation of similarity and complementarity in terms of preferences and transitivity. Some social relations, especially those depending on close bonds such as friendship or trust, are often driven by homophily [42, 47] or preference for connecting to others similar to us (self-preference). This implies transitivity of ties and the abundance of triangles due to triangle closure. However, other relations such as recognition or skill-based collaboration [70] are based on preferences decoupled from the properties of the ego. In this case two nodes with similar preferences connect to the same neighbors but not necessarily to each other. This leads to what can be called second-order transitivity which in turn implies quadrangle closure. **(C)** Biological networks. Majority of networks feature both increased similarity and complementarity indicating higher structural diversity than in the case of social networks. This is consistent with multiple results reporting the abundance of both triangle (e.g. feed-back and feed-forward loops) and quadrangle (e.g. bi-fan and bi-parallel) based motifs [48, 58, 64]. **(D)** Examples of the relationship between directed motifs often reported for biological networks such as gene transcription regulatory networks and undirected motifs used for defining structural similarity and complementarity.

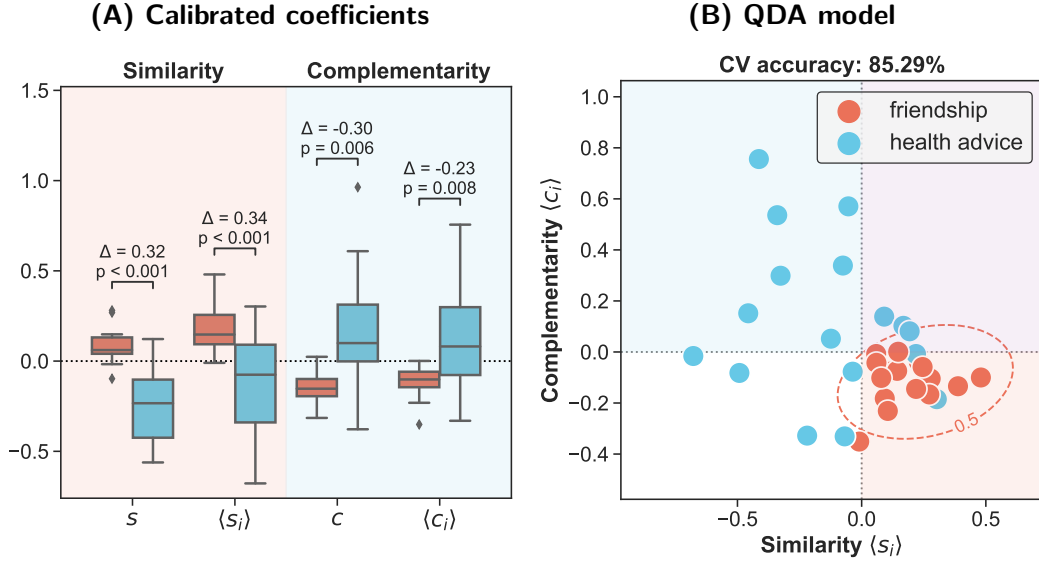


Figure 6. Comparison of structural coefficients between friendship and health advice networks in 17 Ugandan villages. Observed values were calibrated based on 500 samples from UBCM (SI: S5). **(A)** Univariate distributions of global and average node-wise coefficients reveal significant differences between the friendship and health advice networks which are consistent with the hypothesis. The friendship networks feature significantly higher structural similarity and the health advice networks higher complementarity. The average differences between networks from the same villages are denoted by Δ 's. Statistical significance was assessed using one-sample t -test applied to the differences and p -values were adjusted for multiple testing using Holm-Bonferroni method. **(B)** Bivariate distribution of the calibrated values of the average node-wise similarity and complementarity coefficients. The decision boundary separating the friendship and health advice networks (marked in red) is based on Quadratic Discriminant Analysis (QDA). The out-of-sample classification accuracy was estimated with stratified 17-fold cross-validation (one fold per village).

This dataset has the structure of a natural experiment as for each village we have two different networks. Therefore, it provides a perfect setting for testing our hypothesis. Namely, it is sociologically justified to expect the friendship networks to feature high structural similarity as it is a well documented fact that friendship relations are to a large extent shaped by homophily [34, 42, 47]. On the other hand, health advice networks should be at least partially driven by complementarity, as the act of advice is usually based on the recognition of and preference for one's knowledge as well as an information differential between an adviser and an advisee. In other words, advising is based on a synergy between needs and assets of two agents. Moreover, it can be also seen as a particular kind of skill-based collaboration, which is known to be linked to complementarity and heterophily [55, 70]. Thus, it is justified to expect the health advice networks to feature high structural complementarity.

As evident in Fig. 6A, the results are in clear agreement with the theoretical expectations. The similarity coefficients in the friendship networks were typically increased relative to the null model (average log-ratios greater than zero) and significantly higher than in the health advice networks ($p < 0.001$). On the other hand, the results for the complementarity coefficients were exactly opposite and in this case the health advice networks featured significantly larger calibrated values ($p < 0.01$).

Thanks to the convenient quasi-experimental structure of the dataset and the calibration accounting for differences in degree sequences the results provide strong support for the claim that, *ceteris paribus*, social relations based on similarity and complementarity leave distinct structural signatures in social networks which can be detected using structural coefficients. In other words, we showed that, all else being equal, similarity-based ties are linked to the abundance of triangles and those based on complementarities to the abundance of quadrangles. This confirms the theoretical validity of the proposed framework and shows that patterns captured by structural coefficients are indeed related to meaningful domain-specific phenomena. Crucially, it also shows that there are types of social

relations which are driven not by similarity but complementarity, so the default assumption of homophily is not always adequate.

In order to gauge the discriminatory power of the coefficients better, we fitted also a simple supervised classifier based on Quadratic Discriminant Analysis (QDA) [Sec. 4.3 in 28]. To facilitate visualization we used only two predictors: average node-wise similarity and complementarity coefficients. The estimated out-of-sample accuracy was 85.29% (Fig. 6B), which provides further confirmation of the theoretical validity of our approach.

2.6. Structural diversity across the tree of life

Functioning of all biological organisms depends on protein-protein interactions (PPIs), which themselves are constrained by the presence of compatible binding sites [35]. Hence, it can be argued that it is not similar but complementary proteins that are most likely to interact, or that two proteins sharing a neighbor do not have to be connected but instead are likely to share other neighbors (and be structurally equivalent). This view is supported by the statistical over-representation of quadrangle-based motifs in interactome networks [48, 58] as well as recent advances in PPI prediction, which showed that models based on 3-paths (L3) and quadrangle closure outperform those based on 2-paths (L2) and triangle closure [35]. Moreover, there is substantial evidence that protein neighborhoods in interaction networks across the tree of life tend to gradually shift from the dominance of triangles to quadrangles during evolution [74]. Nonetheless, triangle-based motifs are also prevalent in PPI networks and their presence tend to even correlate positively with the abundance of quadrangles [64]. Here we study this problem from the perspective of structural similarity and complementarity and show that increasing complexity of organisms is associated with higher structural diversity of PPI networks, meaning that protein neighborhoods tend to feature increasing numbers of both triangles and quadrangles.

We studied PPI networks, or interactomes, of 1840 species across the tree of life [74] (see Fig. 7 for details). We used network size (number of proteins) for a proxy of the biological complexity of an organism, which is arguably justified as on average interactomes of more complex organisms, such as animals or green plants, are markedly larger than those of bacteria or archaea. Moreover, taxa with larger interactomes on average also tend to have longer average evolution times (Fig. 7B).

The analysis was focused on the structural diversity of protein neighborhoods in terms of the local abundance of triangles and quadrangles in relation to the organism complexity (interactome size). We quantified the structure at the level of entire networks in terms of fractions of nodes with significantly high values of s_i and c_i coefficients or both of them (see Fig. 7 for details). Moreover, we also combined the fractions in a synthetic index of structural diversity, which is defined as follows.

Let $p_S^\alpha(G)$, $p_C^\alpha(G)$, $p_B^\alpha(G)$ and $p_N^\alpha(G)$ be respectively proportions of nodes with significantly high values (at $p \leq \alpha$) of s_i or c_i coefficients or both of them or neither in a graph G . Then, we can define analogous proportions conditioned on the set of nodes with at least one significant value as $p_{X|N'}^\alpha(G) = p_X^\alpha(G)/(1-p_N^\alpha(G))$ for $X = S, C, B$. Together, the conditional proportions define a probability distribution \mathcal{P}_G^α . Finally, the structural diversity index of a graph G at a significance level α is defined as:

$$\mathcal{S}_\alpha(G) = (1 - p_N^\alpha) \mathbb{H}(\mathcal{P}_G^\alpha) \quad (11)$$

where $\mathbb{H}(\cdot)$ is normalized Shannon entropy functional [57]. This measure captures structural heterogeneity of protein neighborhoods while being penalized for networks with mostly random-like structure.

Our analysis (see Fig. 7 for details) indicates a large amount of structural variation between different species and groups of organisms. In particular, it suggests that bacteria interactomes tend to be driven by complementarity, and therefore dominated by quadrangles, to a larger extent than those of other groups. On the other hand, more complex eukaryotes (green plants, fungi and animals) tend to feature nodes with both high structural similarity and complementarity more often, which implies that protein neighborhoods in their interactomes are more heterogeneous and contain both many triangles and quadrangles. Crucially, this intuition is also confirmed by our structural diversity index which correlates positively with organism complexity (interactome size) quite strongly (Fig. 7D). Apart from the tail composed of species with large PPI networks where the trend seems to bifurcate into two groups of organisms with unexpectedly high and low diversity scores (with some notable outliers such as *Homo sapiens* and *Sarcophilus harrisi*, or Tasmanian devil), the model provides a relatively good representation of the data generating process (see additional details and analyses in SI: S7).

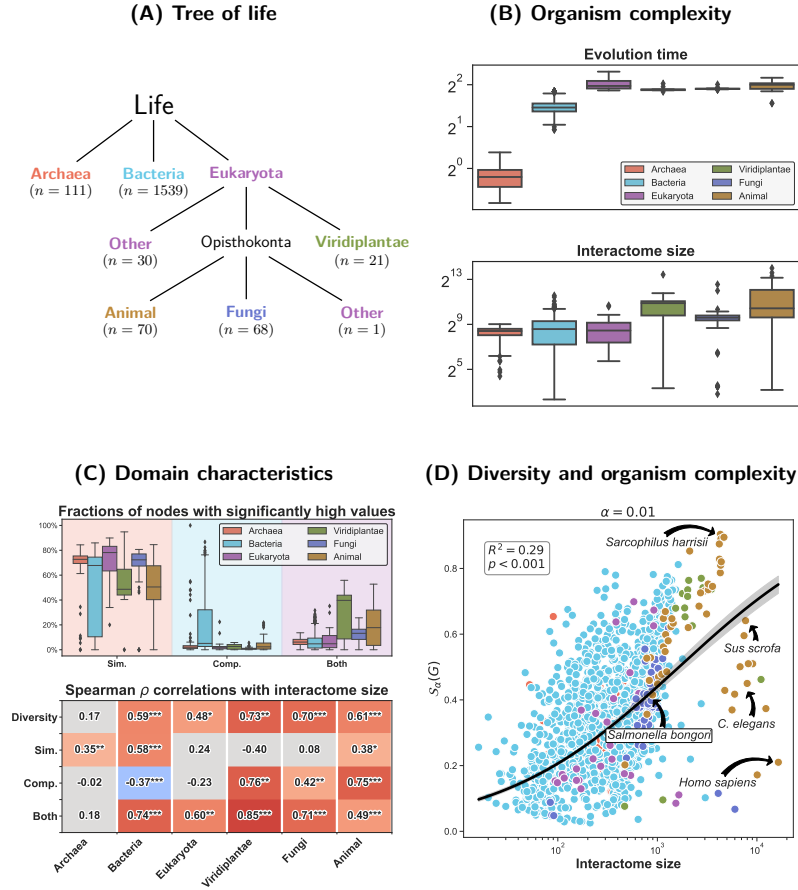


Figure 7. Structural diversity of 1840 interactomes across the tree of life [74] (see Materials and Methods). The analysis was based on proportions of nodes with significantly high values ($p \leq \alpha = 0.01$) of structural coefficients s_i and c_i or both of them. However, we also checked the robustness of the main results for alternative levels $\alpha = 0.05, 0.10$ (SI: S7). Significance was assessed based on null distributions estimated with 100 samples from UBCM (SI: S6). **(A)** Simplified tree of life and the division of organisms into groups. We followed the standard division into the domains of Archaea, Bacteria and Eukaryota [69], but also distinguished three arguably most complex taxa within eukaryotes: green plants (Viridiplantae), fungi and animals (Metazoa). The two “other” classes together form the group of all other eukaryotes. **(B)** Evolution time and interactome sizes in groups. **(C)** General characteristic of the structure of interactomes in different domains/groups. Proportions of nodes with significantly high values of s_i are high in all groups, but in general tend to be much lower among bacteria, which, on the other hand, are the only group that tends to have relatively large numbers of proteins with high values of structural complementarity. Crucially, it is more complex eukaryotes, particularly animals and plants, which feature many nodes with significantly high values of both s_i and c_i . This suggests that interactomes of more complex organisms tend to be more structurally diverse. The lower panel shows monotonic Spearman ρ correlations between interactome size and the proportions as well as the diversity index [11] (** $p \leq 0.001$, ** $p \leq 0.01$, * $p \leq 0.05$; Holm-Bonferroni correction for multiple testing was used). Notably, in all groups except Archaea the correlations between interactome size and the diversity index as well as the “both” proportion are strongly positive. Moreover, complementarity increases with network size in plants, fungi and animals but decreases in bacteria, which means that in both cases the general trend goes in the direction of greater structural diversity. **(D)** Structural diversity [11] and interactome size. We modeled the relationship using linear model with logit transform applied to the diversity index and log transform to the number of nodes. Thus, the relationship between “odds” of the structural coefficient and the number of nodes follows a power law, $S_\alpha(G)/(1 - S_\alpha(G)) \propto n^\gamma$, with $\gamma = 0.48$ (95% CI: [0.45, 0.51]; $p < 0.001$). The general correlation is positive and quite strong (details in SI: S7).

The results suggest a general tendency towards greater structural diversity in PPI networks of more complex organisms. In many cases this implies an increasing prevalence of quadrangles, which is consistent with the results reported in Ref. [74] as well as the general importance of complementarity of binding sites for protein-protein interactions [35]. However, our results also indicate that triangles are still important, perhaps as a manifestation of feed-back and feed-forward loops, and interactomes often feature many triangles and quadrangles at the same time. This suggests a way for improving on PPI prediction models based purely on L2 or L3 [35] measures by using a model averaging combining the two metrics in a way somehow informed by information on the local structure provided by structural coefficients. We leave a detailed exploration of this idea for future work.

3. Discussion

Starting from first principles based on simple geometric arguments we introduced a network theory of similarity- and complementarity-driven relations. We linked both relational principles to their characteristic network motifs — triangles and quadrangles respectively — and defined two general families of structural similarity and complementarity coefficients measuring the extent to which they shape the structure of any given network. In other words, we showed that both similarity and complementarity leave statistically detectable structural signatures, which opens up new possibilities for studying the structure of various networked systems explicitly in terms of the impact of these two relational principles. In particular, to our best knowledge, the principle of complementarity has not been yet operationalized in purely network terms (but see an alternative geometric model proposed in Ref. [33]). Here we filled this gap and showed on multiple empirical examples that complementarity is important for many kinds of social and biological relations.

The proposed family of structural similarity coefficients is built on top of classical local clustering [68] and more recent local closure [71] coefficients. Crucially, it combines these two perspectives in one general measure which captures two different aspects of the fundamental triadic closure process: (1) the tendency of “friends” of ego to connect to each other and (2) the analogous tendency of ego to connect to “friends of its friends”. On the other hand, the family of complementarity coefficients, constructed in the same way but based on counting quadrangles instead of triangles, measures the quadrangle/tetradic closure as well as the presence of locally dense bipartite-like subgraphs. Thus, the coefficients map markedly different structural patterns in networks to generic and interpretable relational principles of similarity and complementarity.

While the prevalence of triangles in many real-world systems, in particular social networks [6, 34], has often been explained in terms of the principle of similarity, or homophily, and a latent network geometry it implies [11, 30, 36, 62], the statistical over-representation of quadrangles (4-cycles or squares) in many systems, such as protein-protein interaction (PPI) networks [35, 64, 74], is less understood, especially in terms of generic principles universal across application domains. Here we showed that the abundance of quadrangles can be explained in terms of complementarity, or differences and synergy, between features of connected nodes and that such relations can be represented geometrically in as natural way as similarity-driven ties.

Using structural coefficients applied to a rich empirical material, we confirmed that typically social relations such as friendship or trust are driven by similarity and therefore are transitive and linked to the abundance of triangles. However, we also showed that some types of relations, for instance recognition, skill-based collaboration or general preference, are more likely to be driven by complementarity, which leads to markedly different structures of social networks dominated by quadrangles instead of triangles. Importantly, this indicates that such relations are not directly transitive ($i \sim j \wedge j \sim k \Rightarrow i \sim k$), but instead second-order transitive ($i \sim j \wedge j \sim k \wedge k \sim l \Rightarrow i \sim l$), which implies that the principle of triangle (2-path) closure does not capture the dynamics of such systems very well. Instead, it is quadrangle (3-path) closure which is more adequate, so the default assumption of homophily/triadic closure [6, 34, 47] is not always justified. Thus, our results encourage more nuanced approaches to social network analysis and potentially can be used to design novel, more flexible link prediction methods.

We also confirmed that biological networks such as gene transcription regulatory or general PPI networks are more likely to be driven by complementarity and feature many quadrangles than typical social networks. This is consistent with multiple empirical results [35, 58, 64, 74] and the general mechanism of protein-protein interactions based on complementarity of binding sites [35]. Using structural coefficients, we demonstrated that interactome networks of more complex organisms across the tree of life tend to be more structurally diverse, meaning that

they consist of many proteins with neighborhoods containing significantly high numbers of both triangles and quadrangles. This indicates a large degree of heterogeneity of structure in PPI networks and suggests that recent results showing that protein interaction prediction based on 3-path (L3) closure is more effective than the 2-path (L2) closure rule [35], could be perhaps further improved by combining the L2 and L3 principles in a way informed by the local structure around a given pair of proteins.

More generally, when edge directions do not play a role or can be ignored, almost all motifs observed commonly across different types of networks, from feed-back loops to so-called bi-fans [48, 58, 64], can be seen as forms of either triangles or quadrangles. Therefore, understanding general principles leading to the emergence of these two fundamental network motifs can help to reveal commonalities between structural and functional properties of different systems across application domains. The principles of complementarity and similarity provide a generic interpretative frame tied to a concrete mathematical operationalization which, we believe, may be very helpful in this respect. Moreover, by defining complementarity in geometric terms, our work may help extend the range of applicability of the emerging field of network geometry [11], which so far has been focused primarily on similarity, to systems driven by differences and synergy.

An important limitation of our work is the fact that our methods currently can be applied only to undirected and unweighted networks. However, generalizing them to the weighted case should be rather straightforward, and we plan to address this problem in the future. In particular, it should be possible to define weighted structural coefficients following the approach used for defining weighted clustering coefficient in Ref. [7]. On the other hand, the geometric motivation of structural coefficients is inherently undirected, so it is not immediately clear how directed coefficients should be defined. For now, we leave it as an interesting open problem.

In summary, we showed that both similarity and complementarity are important organizational principles shaping the structure of social and biological networks, and that they can be linked to interpretable, domain-specific phenomena. We proposed a set of coefficients for measuring the extent to which they shape the structure of networks and demonstrated the theoretical validity and practical utility of the proposed framework on a rich empirical material. Crucially, by introducing a network theory of the principle of complementarity, which has not been yet operationalized in purely network terms, our work extends significantly the set of methods available to network scholars.

4. Materials and methods

4.1. Computing structural coefficients

Structural coefficients are based on counting triples and triangles (similarity) as well as quadruples and quadrangles (complementarity). While the first problem is relatively easy and efficient methods for solving it are implemented in most of popular libraries for graph-theoretical computations, the second problem of counting quadruples and quadrangles is more difficult and corresponding efficient algorithms are not widely known. Here we solve both problems by counting all motifs of interest at the level of individual edges and then aggregate the edge-wise counts to node-wise or global counts when necessary. We propose an algorithm which can be seen as a special case of the state-of-the-art graphlet counting method proposed in Ref. [1]. We call it **PathCensus** algorithm as ultimately it counts how often different types of paths and cycles occur in a given network. Pseudocode for the algorithm and other computational details are discussed in the SI: S3.

4.2. pathcensus package

We implemented all the methods and algorithms for calculating structural coefficients as well as several other utilities including most appropriate null models and auxiliary methods for conducting statistical inference in **pathcensus** package for Python. The core routines are just-in-time compiled to highly optimized C code using *Numba* library [38] ensuring high efficiency. The package has an extensive documentation including several usage examples. It will be distributed through *Python Package Index* upon publication.

4.3. Network datasets

All network datasets used in this paper were downloaded from the Netzscheider network repository [52]. In all analyses only largest connected components were used and networks were simplified by removing multilinks and self-loops. Moreover, in the case of directed or weighted networks edge directions and weights were ignored. See the SI: S8 for details.

Acknowledgments

We thank Shlomo Havlin for very useful advice on contextualizing our work within the literature on network motifs as well as Brennan Klein and Ivan Voitalov for an inspiring conversation on complementarity-driven relations few years ago. We also thank Maciej Talaga for proofreading and Mikołaj Biesaga for the help with testing the code.

Funding

This work was supported by a grant from Polish National Science Center (*Outline of a network-geometric theory of social structure*, 2020/37/N/HS6/00796).

Author contributions

S.T. and A.N. conceptualized the project. S.T. formulated the mathematical formalism and wrote the related proofs, designed the algorithms and developed their Python implementation in the form of `pathcensus` package. S.T. conducted the data analyses and prepared the figures. S.T. and A.N. wrote the main text together.

Competing interests

The authors declare no competing interests.

Data and materials availability

Data and code needed for reproducing the analyses presented in the paper will be made freely available as a *Github* repository and `pathcensus` package will be released at *Python Package Index* upon publication.

References

- [1] Nesreen K. Ahmed, Jennifer Neville, Ryan A. Rossi, and Nick Duffield. 2015. Efficient Graphlet Counting for Large Networks. In *2015 IEEE International Conference on Data Mining*. IEEE, Atlantic City, NJ, USA, 1–10. <https://doi.org/10.1109/ICDM.2015.141>
- [2] Emanuele Aliverti and Daniele Durante. 2019. Spatial Modeling of Brain Connectivity Data via Latent Distance Models with Nodes Clustering. *Statistical Analysis and Data Mining: The ASA Data Science Journal* 12, 3 (2019), 185–196. <https://doi.org/10.1002/sam.11412>
- [3] Uri Alon. 2007. Network Motifs: Theory and Experimental Approaches. *Nature Reviews Genetics* 8, 6 (2007), 450–461. <https://doi.org/10.1038/nrg2102>
- [4] Aris Anagnostopoulos, Ravi Kumar, and Mohammad Mahdian. 2008. Influence and Correlation in Social Networks. In *Proceeding of the 14th ACM SIGKDD International Conference on Knowledge Discovery and Data Mining*. ACM Press, Las Vegas, Nevada, USA, 7–15. <https://doi.org/10.1145/1401890.1401897>
- [5] S. Aral, L. Muchnik, and A. Sundararajan. 2009. Distinguishing Influence-Based Contagion from Homophily-Driven Diffusion in Dynamic Networks. *Proceedings of the National Academy of Sciences* 106, 51 (2009), 21544–21549. <https://doi.org/10.1073/pnas.0908800106>

- [6] Aili Asikainen, Gerardo Iñiguez, Javier Ureña-Carrión, Kimmo Kaski, and Mikko Kivelä. 2020. Cumulative Effects of Triadic Closure and Homophily in Social Networks. *Science Advances* 6, 19 (2020), eaax7310. <https://doi.org/10.1126/sciadv.aax7310>
- [7] A. Barrat, M. Barthélemy, R. Pastor-Satorras, and A. Vespignani. 2004. The Architecture of Complex Weighted Networks. *Proceedings of the National Academy of Sciences* 101, 11 (2004), 3747–3752. <https://doi.org/10.1073/pnas.0400087101>
- [8] Yoav Benjamini, Abba M. Krieger, and Daniel Yekutieli. 2006. Adaptive Linear Step-up Procedures That Control the False Discovery Rate. *Biometrika* 93, 3 (2006), 491–507. <https://doi.org/10.1093/biomet/93.3.491>
- [9] T. Beuming, L. Skrabanek, M. Y. Niv, P. Mukherjee, and H. Weinstein. 2005. PDZBase: A Protein-Protein Interaction Database for PDZ-domains. *Bioinformatics* 21, 6 (2005), 827–828. <https://doi.org/10.1093/bioinformatics/bti098>
- [10] Peter M. Blau. 1977. *Inequality and Heterogeneity: A Primitive Theory of Social Structure*. The Free Press.
- [11] Marián Boguñá, Ivan Bonamassa, Manlio De Domenico, Shlomo Havlin, Dmitri Krioukov, and M. Ángeles Serrano. 2021. Network Geometry. *Nature Reviews Physics* 3, 2 (2021), 114–135. <https://doi.org/10.1038/s42254-020-00264-4>
- [12] Marián Boguñá, Dmitri Krioukov, Pedro Almagro, and M. Ángeles Serrano. 2020. Small Worlds and Clustering in Spatial Networks. *Physical Review Research* 2, 2 (2020). <https://doi.org/10.1103/PhysRevResearch.2.023040>
- [13] Marián Boguñá, Fragkiskos Papadopoulos, and Dmitri Krioukov. 2010. Sustaining the Internet with Hyperbolic Mapping. *Nature Communications* 1, 1 (2010), 62. <https://doi.org/10.1038/ncomms1063>
- [14] Pierre Bourdieu. 1986. *Distinction : A Social Critique of the Judgement of Taste*. Routledge. <https://doi.org/10.4324/9780203720790>
- [15] Goylette F. Chami, Sebastian E. Ahnert, Narcis B. Kabatereine, and Edridah M. Tukahebwa. 2017. Social Network Fragmentation and Community Health. *Proceedings of the National Academy of Sciences* 114, 36 (2017), E7425–E7431. <https://doi.org/10.1073/pnas.1700166114>
- [16] Seungwha Chung, Harbir Singh, and Kyungmook Lee. 2000. Complementarity, Status Similarity and Social Capital as Drivers of Alliance Formation. *Strategic Management Journal* 21 (2000), 1–22. [https://doi.org/10.1002/\(SICI\)1097-0266\(200001\)21:1<1::AID-SMJ63>3.0.CO;2-P](https://doi.org/10.1002/(SICI)1097-0266(200001)21:1<1::AID-SMJ63>3.0.CO;2-P)
- [17] James Coleman, Elihu Katz, and Herbert Mentzel. 1957. The Diffusion of an Innovation Among Physicians. *Sociometry* 20, 4 (1957), 253–270.
- [18] Sean R. Collins, Patrick Kemmeren, Xue-Chu Zhao, Jack F. Greenblatt, Forrest Spencer, Frank C.P. Holstege, Jonathan S. Weissman, and Nevan J. Krogan. 2007. Toward a Comprehensive Atlas of the Physical Interactome of *Saccharomyces Cerevisiae*. *Molecular & Cellular Proteomics* 6, 3 (2007), 439–450. <https://doi.org/10.1074/mcp.M600381-MCP200>
- [19] Stéphane Coulomb, Michel Bauer, Denis Bernard, and Marie-Claude Marsolier-Kergoat. 2005. Gene Essentiality and the Topology of Protein Interaction Networks. *Proceedings of the Royal Society B: Biological Sciences* 272, 1573 (2005), 1721–1725. <https://doi.org/10.1098/rspb.2005.3128>
- [20] Wouter de Nooy. 1999. A Literary Playground: Literary Criticism and Balance Theory. *Poetics* 26, 5-6 (1999), 385–404. [https://doi.org/10.1016/S0304-422X\(99\)00009-1](https://doi.org/10.1016/S0304-422X(99)00009-1)
- [21] Kurt Dopfer, Jason Potts, and Andreas Pyka. 2016. Upward and Downward Complementarity: The Meso Core of Evolutionary Growth Theory. *Journal of Evolutionary Economics* 26, 4 (2016), 753–763. <https://doi.org/10.1007/s00191-015-0434-4>

- [22] Paul Erdős and Alfred Rényi. 1959. On Random Graphs I. *Publicationes Mathematicae* 6 (1959), 290–297.
- [23] Rob M Ewing, Peter Chu, Fred Elisma, Li Hongyan, Paul Taylor, Shane Climie, Linda McBroom-Cerajewski, Mark D Robinson, Liam O’Connor, Michael Li, Rod Taylor, Moyez Dharsee, Yuen Ho, Adrian Heilbut, Lynda Moore, Shudong Zhang, Olga Ornatsky, Yury V Bukhman, Martin Ethier, Yinglun Sheng, Julian Vasilescu, Mohamed Abu-Farha, Jean-Philippe Lambert, Henry S Duwel, Ian I Stewart, Bonnie Kuehl, Kelly Hogue, Karen Colwill, Katharine Gladwish, Brenda Muskat, Robert Kinach, Adams Sally-Lin, Michael F Moran, Gregg B Morin, Thodoros Topaloglou, and Daniel Figeys. 2007. Large-Scale Mapping of Human Protein–Protein Interactions by Mass Spectrometry. *Molecular Systems Biology* 3, 1 (2007), 89. <https://doi.org/10.1038/msb4100134>
- [24] Michael Fire and Rami Puzis. 2016. Organization Mining Using Online Social Networks. *Networks and Spatial Economics* 16, 2 (2016), 545–578. <https://doi.org/10.1007/s11067-015-9288-4>
- [25] L Freeman, S Freeman, and A Michaelson. 1988. On Human Social Intelligence. *Journal of Social and Biological Systems* 11, 4 (1988), 415–425. [https://doi.org/10.1016/0140-1750\(88\)90080-2](https://doi.org/10.1016/0140-1750(88)90080-2)
- [26] Linton C Freeman, Cynthia M Webster, and Deirdre M Kirke. 1998. Exploring Social Structure Using Dynamic Three-Dimensional Color Images. *Social Networks* 20, 2 (1998), 109–118. [https://doi.org/10.1016/S0378-8733\(97\)00016-6](https://doi.org/10.1016/S0378-8733(97)00016-6)
- [27] Ranjay Gulati. 1995. Social Structure and Alliance Formation Patterns: A Longitudinal Analysis. *Administrative Science Quarterly* 40, 4 (1995), 619. <https://doi.org/10.2307/2393756>
- [28] Trevor Hastie, Robert Tibshirani, and Jerome Friedman. 2008. *The Elements of Statistical Learning* (second ed.). Springer.
- [29] Desmond J. Higham, Marija Rašajski, and Nataša Pržulj. 2008. Fitting a Geometric Graph to a Protein–Protein Interaction Network. *Bioinformatics* 24, 8 (2008), 1093–1099. <https://doi.org/10.1093/bioinformatics/btn079>
- [30] Peter D Hoff, Adrian E Raftery, and Mark S Handcock. 2002. Latent Space Approaches to Social Network Analysis. *J. Amer. Statist. Assoc.* 97, 460 (2002), 1090–1098. <https://doi.org/10.1198/016214502388618906>
- [31] Mingshan Jia, Bogdan Gabrys, and Katarzyna Musial. 2021. Measuring Quadrangle Formation in Complex Networks. *IEEE Transactions on Network Science and Engineering* (2021), 1–1. <https://doi.org/10.1109/TNSE.2021.3123735>
- [32] G. Joshi-Tope. 2004. Reactome: A Knowledgebase of Biological Pathways. *Nucleic Acids Research* 33, Database issue (2004), D428–D432. <https://doi.org/10.1093/nar/gki072>
- [33] Maksim Kitsak. 2020. Latent Geometry for Complementarity-Driven Networks. *arXiv:2003.06665 [cond-mat, physics:physics]* (2020). arXiv:cond-mat, physics:physics/2003.06665
- [34] Gueorgi Kossinets and D. J. Watts. 2009. Origins of Homophily in an Evolving Social Network. *Amer. J. Sociology* 115, 2 (2009), 405–450. <https://doi.org/10.1086/599247>
- [35] István A. Kovács, Katja Luck, Kerstin Spirohn, Yang Wang, Carl Pollis, Sadie Schlabach, Wenting Bian, Dae-Kyum Kim, Nishka Kishore, Tong Hao, Michael A. Calderwood, Marc Vidal, and Albert-László Barabási. 2019. Network-Based Prediction of Protein Interactions. *Nature Communications* 10, 1 (2019), 1240. <https://doi.org/10.1038/s41467-019-09177-y>
- [36] Dmitri Krioukov. 2016. Clustering Implies Geometry in Networks. *Physical Review Letters* 116, 20 (2016). <https://doi.org/10.1103/PhysRevLett.116.208302>
- [37] Pavel N. Krivitsky, Mark S. Handcock, Adrian E. Raftery, and Peter D. Hoff. 2009. Representing Degree Distributions, Clustering, and Homophily in Social Networks with Latent Cluster Random Effects Models. *Social Networks* 31, 3 (2009), 204–213. <https://doi.org/10.1016/j.socnet.2009.04.001>

- [38] Siu Kwan Lam, Antoine Pitrou, and Stanley Seibert. 2015. Numba: A LLVM-based Python JIT Compiler. In *Proceedings of the Second Workshop on the LLVM Compiler Infrastructure in HPC - LLVM '15*. ACM Press, Austin, Texas, 1–6. <https://doi.org/10.1145/2833157.2833162>
- [39] E. L. Lehmann and George Casella. 1998. *Theory of Point Estimation* (2nd ed ed.). Springer, New York.
- [40] Benjamin F. Maier and Dirk Brockmann. 2017. Cover Time for Random Walks on Arbitrary Complex Networks. *Physical Review E* 96, 4 (2017), 042307. <https://doi.org/10.1103/PhysRevE.96.042307>
- [41] Patrick M. Markey and Charlotte N. Markey. 2007. Romantic Ideals, Romantic Obtainment, and Relationship Experiences: The Complementarity of Interpersonal Traits among Romantic Partners. *Journal of Social and Personal Relationships* 24, 4 (2007), 517–533. <https://doi.org/10.1177/0265407507079241>
- [42] Peter V. Marsden. 1988. Homogeneity in Confiding Relations. *Social Networks* 10, 1 (1988), 57–76. [https://doi.org/10.1016/0378-8733\(88\)90010-X](https://doi.org/10.1016/0378-8733(88)90010-X)
- [43] Paolo Massa, Martino Salvetti, and Danilo Tomasoni. 2009. Bowling Alone and Trust Decline in Social Network Sites. In *2009 Eighth IEEE International Conference on Dependable, Autonomic and Secure Computing*. IEEE, Chengdu, China.
- [44] Carolina E. S. Mattsson, Frank W. Takes, Eelke M. Heemskerk, Cees Diks, Gert Buiten, Albert Faber, and Peter M. A. Sloot. 2021. Functional Structure in Production Networks. *Frontiers in Big Data* 4 (2021), 666712. <https://doi.org/10.3389/fdata.2021.666712>
- [45] Julian McAuley and Jure Leskovec. 2012. Learning to Discover Social Circles in Ego Networks. In *Advances in Neural Information Processing Systems*, Vol. 25. Curran Associates, Inc.
- [46] J. M. McPherson. 2004. A Blau Space Primer: Prolegomenon to an Ecology of Affiliation. *Industrial and Corporate Change* 13, 1 (2004), 263–280. <https://doi.org/10.1093/icc/13.1.263>
- [47] J. M. McPherson, L. Smith-Lovin, and J. M. Cook. 2001. Birds of a Feather: Homophily in Social Networks. *Annual Review of Sociology* 27, 1 (2001), 415–444. <https://doi.org/10.1146/annurev.soc.27.1.415>
- [48] R. Milo, S. Shen-Orr, S. Itzkovitz, N. Kashtan, D. Chklovskii, and Uri Alon. 2002. Network Motifs: Simple Building Blocks of Complex Networks. *Science* 298, 5594 (2002), 824–827. <https://doi.org/10.1126/science.298.5594.824>
- [49] M. E. J. Newman. 2010. *Networks: An Introduction*. Oxford University Press, Oxford, New York.
- [50] Tore Opsahl. 2013. Triadic Closure in Two-Mode Networks: Redefining the Global and Local Clustering Coefficients. *Social Networks* 35, 2 (2013), 159–167. <https://doi.org/10.1016/j.socnet.2011.07.001>
- [51] Fragkiskos Papadopoulos, Rodrigo Aldecoa, and Dmitri Krioukov. 2015. Network Geometry Inference Using Common Neighbors. *Physical Review E* 92, 2 (2015), 022807. <https://doi.org/10.1103/PhysRevE.92.022807> arXiv:1502.05578
- [52] Tiago P. Peixoto. 2020. The Netzscheleuder Network Catalogue and Repository. <https://networks.skewed.de/>.
- [53] Matthew Richardson, Rakesh Agrawal, and Pedro Domingos. 2003. Trust Management for the Semantic Web. In *The Semantic Web - ISWC 2003 (Lecture Notes in Computer Science)*, Dieter Fensel, Katia Sycara, and John Mylopoulos (Eds.). Springer, Berlin, Heidelberg, 351–368. https://doi.org/10.1007/978-3-540-39718-2_23
- [54] Oliver Richters and Tiago P. Peixoto. 2011. Trust Transitivity in Social Networks. *PLoS ONE* 6, 4 (2011), e18384. <https://doi.org/10.1371/journal.pone.0018384>

- [55] Mark T. Rivera, Sara B. Soderstrom, and Brian Uzzi. 2010. Dynamics of Dyads in Social Networks: Assortative, Relational, and Proximity Mechanisms. *Annual Review of Sociology* 36, 1 (2010), 91–115. <https://doi.org/10.1146/annurev.soc.34.040507.134743>
- [56] Jean-François Rual, Kavitha Venkatesan, Tong Hao, Tomoko Hirozane-Kishikawa, Amélie Dricot, Ning Li, Gabriel F. Berriz, Francis D. Gibbons, Matija Dreze, Nono Ayivi-Guedehoussou, Niels Klitgord, Christophe Simon, Mike Boxem, Stuart Milstein, Jennifer Rosenberg, Debra S. Goldberg, Lan V. Zhang, Sharyl L. Wong, Giovanni Franklin, Siming Li, Joanna S. Albala, Janghoo Lim, Carlene Fraughton, Estelle Llamosas, Sebiha Cevik, Camille Bex, Philippe Lamesch, Robert S. Sikorski, Jean Vandenhoute, Huda Y. Zoghbi, Alex Smolyar, Stephanie Bosak, Reynaldo Sequerra, Lynn Doucette-Stamm, Michael E. Cusick, David E. Hill, Frederick P. Roth, and Marc Vidal. 2005. Towards a Proteome-Scale Map of the Human Protein-Protein Interaction Network. *Nature* 437, 7062 (2005), 1173–1178. <https://doi.org/10.1038/nature04209>
- [57] Claude Shannon. 1948. A Mathematical Theory of Communication. *Bell System Technical Journal* 27, 3 (1948), 379–423.
- [58] Shai S. Shen-Orr, Ron Milo, Shmoolik Mangan, and Uri Alon. 2002. Network Motifs in the Transcriptional Regulation Network of Escherichia Coli. *Nature Genetics* 31, 1 (2002), 64–68. <https://doi.org/10.1038/ng881>
- [59] Tiziano Squartini, Rossana Mastrandrea, and Diego Garlaschelli. 2015. Unbiased Sampling of Network Ensembles. *New Journal of Physics* 17, 2 (2015), 023052. <https://doi.org/10.1088/1367-2630/17/2/023052>
- [60] Pulipati Srilatha and Ramakrishnan Manjula. 2016. Similarity Index Based Link Prediction Algorithms in Social Networks: A Survey. *Journal of Telecommunications and Information Technology* 2 (2016), 87–94.
- [61] Ulrich Stelzl, Uwe Worm, Maciej Lalowski, Christian Haenig, Felix H. Brembeck, Heike Goehler, Martin Stroedicke, Martina Zenkner, Anke Schoenherr, Susanne Koeppen, Jan Timm, Sascha Mintzlaff, Claudia Abraham, Nicole Bock, Silvia Kietzmann, Astrid Goedde, Engin Toksöz, Anja Droege, Sylvia Krobitsch, Bernhard Korn, Walter Birchmeier, Hans Lehrach, and Erich E. Wanker. 2005. A Human Protein-Protein Interaction Network: A Resource for Annotating the Proteome. *Cell* 122, 6 (2005), 957–968. <https://doi.org/10.1016/j.cell.2005.08.029>
- [62] Szymon Talaga and Andrzej Nowak. 2020. Homophily as a Process Generating Social Networks: Insights from Social Distance Attachment Model. *Journal of Artificial Societies and Social Simulation* 23, 2 (2020), 6. <https://doi.org/10.18564/jasss.4252>
- [63] Yu Tian, Sebastian Lautz, Alisdair O. G. Wallis, and Renaud Lambiotte. 2021. Extracting Complements and Substitutes from Sales Data: A Network Perspective. *EPJ Data Science* 10, 1 (2021), 45. <https://doi.org/10.1140/epjds/s13688-021-00297-4>
- [64] Ngoc Hieu Tran, Kwok Pui Choi, and Louxin Zhang. 2013. Counting Motifs in the Human Interactome. *Nature Communications* 4, 1 (2013), 2241. <https://doi.org/10.1038/ncomms3241>
- [65] Nicolò Vallerano, Matteo Bruno, Emiliano Marchese, Giuseppe Trapani, Fabio Saracco, Giulio Cimini, Mario Zanon, and Tiziano Squartini. 2021. Fast and Scalable Likelihood Maximization for Exponential Random Graph Models with Local Constraints. *Scientific Reports* 11, 1 (2021), 15227. <https://doi.org/10.1038/s41598-021-93830-4>
- [66] Remco van der Hofstad, Johan S. H. van Leeuwen, and Clara Stegehuis. 2018. Triadic Closure in Configuration Models with Unbounded Degree Fluctuations. *Journal of Statistical Physics* 173, 3-4 (2018), 746–774. <https://doi.org/10.1007/s10955-018-1952-x>
- [67] Stanley Wasserman and Katherine Faust. 1994. *Social Network Analysis: Methods and Applications*. Cambridge University Press, Cambridge; New York.

- [68] D. J. Watts and S. H. Strogatz. 1998. Collective Dynamics of ‘Small-World’ Networks. *Nature* 393, 6684 (1998), 440. <https://doi.org/10.1038/30918>
- [69] Carl R Woese, Otto Kandler, and Mark Wheelis. 1990. Towards a Natural System of Organisms: Proposal for the Domains Archaea, Bacteria, and Eucarya. *Proceedings of the National Academy of Sciences* 87 (1990), 4576–4579.
- [70] Wen-Jie Xie, Ming-Xia Li, Zhi-Qiang Jiang, Qun-Zhao Tan, Boris Podobnik, Wei-Xing Zhou, and H. Eugene Stanley. 2016. Skill Complementarity Enhances Heterophily in Collaboration Networks. *Scientific Reports* 6, 1 (2016). <https://doi.org/10.1038/srep18727>
- [71] Hao Yin, Austin R. Benson, and Jure Leskovec. 2019. The Local Closure Coefficient: A New Perspective On Network Clustering. In *Proceedings of the Twelfth ACM International Conference on Web Search and Data Mining*. ACM, Melbourne VIC Australia, 303–311. <https://doi.org/10.1145/3289600.3290991>
- [72] Wayne W. Zachary. 1977. An Information Flow Model for Conflict and Fission in Small Groups. *Journal of Anthropological Research* 33, 4 (1977), 452–473. <https://doi.org/10.1086/jar.33.4.3629752>
- [73] Peng Zhang, Jinliang Wang, Xiaojia Li, Menghui Li, Zengru Di, and Ying Fan. 2008. Clustering Coefficient and Community Structure of Bipartite Networks. *Physica A: Statistical Mechanics and its Applications* 387, 27 (2008), 6869–6875. <https://doi.org/10.1016/j.physa.2008.09.006>
- [74] Marinka Zitnik, Rok Sosič, Marcus W. Feldman, and Jure Leskovec. 2019. Evolution of Resilience in Protein Interactomes across the Tree of Life. *Proceedings of the National Academy of Sciences* 116, 10 (2019), 4426–4433. <https://doi.org/10.1073/pnas.1818013116>

Supplementary Information

S1. Similarity and structural equivalence

Here we derive the relationship between similarity coefficient s_{ij} and s_i and structural equivalence. First, we show that s_i is a weighted average of the node-wise coefficients s_{ij} ’s for $j \in \mathcal{N}_1(i)$, that is:

$$s_i = \frac{4T_i}{t_i^W + t_i^H} = \frac{\sum_j (t_{ij}^W + t_{ij}^H) s_{ij}}{\sum_j t_{ij}^W + t_{ij}^H} \quad (\text{S1})$$

Note that Eq. (4) implies that $(t_{ij}^W + t_{ij}^H) s_{ij} = 2T_{ij}$. Moreover, since each triangle including i is shared with two other nodes we have that:

$$\sum_{j \in \mathcal{N}_1(i)} (t_{ij}^W + t_{ij}^H) s_{ij} = \sum_{j \in \mathcal{N}_1(i)} 2T_{ij} = 4T_i \quad (\text{S2})$$

On the other hand, $t_{ij}^W + t_{ij}^H$ is the number of 2-paths traversing the (i, j) edges so it can be written as $t_{ij}^W + t_{ij}^H = d_i + d_j - 2$. Hence, it is easy to see that:

$$\begin{aligned} \sum_{j \in \mathcal{N}_1(i)} t_{ij}^W + t_{ij}^H &= \sum_{j \in \mathcal{N}_1(i)} (d_i + d_j - 2) \\ &= d_i(d_i - 1) + \sum_{j \in \mathcal{N}_1(i)} (d_j - 1) \\ &= t_i^W + t_i^H \end{aligned} \quad (\text{S3})$$

Finally, substituting (S2) and (S3) into (S1) we confirm the desired equality.

Now, we use a common definition of structural equivalence in terms of the Sørensen Index (normalized Hamming similarity) and note its direct connection to our notion of edge-wise structural similarity s_{ij} :

$$H_{ij} = \frac{2n_{ij}}{d_i + d_j} = \frac{2T_{ij}}{d_i + d_j} = s_{ij} \frac{d_i + d_j - 2}{d_i + d_j} \quad (\text{S4})$$

The above implies that $H_{ij} < s_{ij}$ for all (i, j) edges for which s_{ij} is defined. And since we established that s_i is a weighted average of s_{ij} 's with $j \in \mathcal{N}_1(i)$ we have that:

$$\min_j H_{ij} < \min_j s_{ij} \leq s_i \leq \max_j s_{ij} = \max_j \left(H_{ij} \frac{d_i + d_j - 2}{d_i + d_j} \right) \quad (\text{S5})$$

Note that for large values of $d_i + d_j$ the above is approximately equivalent to:

$$\min_j H_{ij} < s_i \leq \max_j H_{ij} \quad (\text{S6})$$

In other words, we showed that the similarity coefficient of a node i is approximately bounded between minimum and maximum structural equivalence (Sørensen Index) between itself and any of its neighbors. Crucially, this also explains why structural similarity is inherently linked to transitivity. If neighbors of i are highly structurally equivalent to it, then it must be very likely that if $i \sim j$ and $j \sim k$ then $i \sim k$.

S2. Complementarity and structural equivalence

Here we derive the relationship between complementarity coefficients c_{ij} and c_i and structural equivalence. We start by showing that c_i is a weighted average of the edge-wise coefficients c_{ij} 's for $j \in \mathcal{N}_1(i)$, that is:

$$c_i = \frac{4Q_{ij}}{q_i^W + q_i^H} = \frac{\sum_j (q_{ij}^W + q_{ij}^H) c_{ij}}{\sum_j q_{ij}^W + q_{ij}^H} \quad (\text{S7})$$

Using Eq. (9) from the Main Text we can write $2Q_{ij} = (q_{ij}^W + q_{ij}^H) c_{ij}$. Moreover, each strong quadrangle including a node i is shared with exactly two other nodes. Hence, we have that:

$$\sum_{j \in \mathcal{N}_1(i)} (q_{ij}^W + q_{ij}^H) c_{ij} = \sum_{j \in \mathcal{N}_1(i)} 2Q_{ij} = 4Q_i \quad (\text{S8})$$

Next, note that each 3-path starting at an (i, j) edge defines a unique ordered quadruple of the form (i, j, k, l) or (j, i, k, l) . The first form is counted as a head quadruple of the node i and a wedge quadruple of the node j and in the second case the order is reversed. And since $q_{ij}^W + q_{ij}^H$ is the number of 3-paths starting at the (i, j) edge it must hold that the:

$$\sum_{j \in \mathcal{N}_1(i)} (q_{ij}^W + q_{ij}^H) = q_i^W + q_i^H \quad (\text{S9})$$

Finally, note that (S8) and (S9) jointly mean that (S7) must be true. As a result, for $j \in \mathcal{N}_1(i)$ we have that:

$$\min_j c_{ij} \leq c_i \leq \max_j c_{ij} \quad (\text{S10})$$

Now, in order to derive the connection between complementarity coefficients and structural equivalence we need first to introduce one additional quantity. For a connected triple (k, i, j) we define *Asymmetric Excess Sørensen Index*:

$$H_{kj|i} = \frac{n_{jk} - 1}{d_k - 1 - a_{jk}} \quad (\text{S11})$$

which measures how many of the connections of k are also shared by j while disregarding edges (i, k) , (i, j) and (j, k) . Note that the excess degree of k is used in the denominator as the (i, k) link needs to be ignored. Moreover,

a_{jk} term accounts for the possible presence of the (j, k) link. Finally, 1 is subtracted from n_{jk} to account for the fact that i is a shared neighbor of j and k .

Next, we also need to use the notion of weak quadrangles allowing for any number of chordal edges. Let $W_{ij} \geq Q_{ij}$ be the number of quadrangles with any number of chords incident to the (i, j) edge. We also define weak edge-wise complementarity to be $h_{ij} = W_{ij}/(q_{ij}^W + q_{ij}^H) \geq c_{ij}$. It is easy to see that:

$$W_{ij} = \sum_{k \in \mathcal{N}_1(i) - \{j\}} n_{jk} - 1 \quad (\text{S12})$$

On the other hand, the number of 3-paths starting at the (i, j) edge is:

$$\begin{aligned} q_{ij}^W + q_{ij}^H &= \sum_{k \in \mathcal{N}_1(i) - \{j\}} (d_k - 1) + \sum_{l \in \mathcal{N}_1(j) - \{i\}} (d_l - 1) - 2n_{ij} \\ &= \sum_{k \in \mathcal{N}_1(i) - \{j\}} (d_k - 1 - a_{jk}) + \sum_{l \in \mathcal{N}_1(j) - \{i\}} (d_l - 1 - a_{il}) \end{aligned} \quad (\text{S13})$$

since q_{ij}^W is the number of (j, i, k, l) and q_{ij}^H of (i, j, k, l) quadruples. The second equality comes from the fact that $n_{ij} = \sum_k a_{jk} = \sum_l a_{il}$. Now, we can use (S11), (S12) and (S13) to rewrite the weak edge-wise complementarity as:

$$h_{ij} = \frac{\sum_k (d_k - 1 - a_{jk}) H_{kj|i} + \sum_l (d_l - 1 - a_{il}) H_{li|j}}{\sum_k (d_k - 1 - a_{jk}) + \sum_l (d_l - 1 - a_{il})} \quad (\text{S14})$$

As a result we have that:

$$\min_{k,l} (H_{kj|i}, H_{li|j}) \leq h_{ij} \leq \max_{k,l} (H_{kj|i}, H_{li|j}) \quad (\text{S15})$$

Using (S10) we can write:

$$\min_{j,k,l} (H_{kj|i}, H_{li|j}) \leq h_i \leq \max_{j,k,l} (H_{kj|i}, H_{li|j}) \quad (\text{S16})$$

Finally, since by definition $c_{ij} \leq h_{ij}$ this implies:

$$0 \leq c_{ij} \leq \max_{k,l} (H_{kj|i}, H_{li|j}) \quad (\text{S17})$$

as well as:

$$0 \leq c_i \leq \max_{j,k,l} (H_{kj|i}, H_{li|j}) \quad (\text{S18})$$

In other words, we just showed that the structural complementarity coefficient defined for a node i is bounded from above by the maximum Asymmetric Excess Sørensen Index between any two of its neighbors or itself and any neighbor of its neighbors. Intuitively, high complementarity can exist only in the presence of high structural equivalence between neighbors of i as well as i and neighbors of its neighbors. Moreover, in the weak case we also have a lower bound of the same nature. We leave a more detailed analysis of the notion of weak complementarity for future work.

Crucially, this explains in what sense complementarity-driven relations are not transitive but yet localized. The principle of complementarity enforces a degree of structural equivalence in the neighborhood of i which in turn induces a particular kind of correlations between the connections of i and its 1- and 2-hop neighbors.

S3. Structural coefficients and PathCensus

S3.1. Formulas and algorithm

Edge-level counts of triples, quadruples, triangles and quadrangles are computed with the algorithm S1. Node and global counts can be obtained by aggregating edge counts. The rules of aggregation are summarized in Table S1. Table S2 presents detailed formulas for all structural coefficients expressed in terms of the aggregated counts.

Algorithm S1. PathCensus algorithm. It takes an undirected graph $G = (V, E)$ with $|V| = n$ and $|E| = m$ as input and returns an array of edge-wise counts of wedge and head triples and quadruples as well as triangles and (strong) quadrangles. For better performance E can be defined (without loss of generality) to ensure that for all edges (i, j) it holds that $d_i \leq d_j$.

```

1: Initialize empty  $C$  ▷  $m \times 8$  array for storing path counts
2: Initialize  $R$  such that  $R_i = 0 \quad \forall i \in V$  ▷  $n \times 1$  array for keeping track of node roles
3: Let  $D$  be the degree sequence of  $G$  ▷  $n \times 1$  array
4: Initialize  $u = 0$ 
5: for  $e = (i, j) \in E$  do ▷ the loop may be parallelized
6:   Set  $u = u + 1$ 
7:   Initialize  $T_{ij}, t_{ij}^W, t_{ij}^H = 0$  ▷ counts of triangles and wedge and head triples
8:   Initialize  $Q_{ij}, q_{ij}^W, q_{ij}^H = 0$  ▷ counts of strong quadrangles and wedge and head quadruples
9:   Initialize  $\text{Star}_i, \text{Star}_j, \text{Tri}_{ij} = \emptyset$  ▷ Empty sets for keeping track of nodes with different roles
10:  for  $(k \neq j) \in \mathcal{N}_1(i)$  do
11:    Add  $k$  to  $\text{Star}_i$  and set  $R_k = 1$ 
12:    Set  $t_{ij}^W = t_{ij}^W + 1$ 
13:  for  $(k \neq i) \in \mathcal{N}_1(j)$  do
14:    if  $R_k = 1$  then
15:       $T_{ij} = T_{ij} + 1$ 
16:      Remove  $k$  from  $\text{Star}_i$ , add  $k$  to  $\text{Tri}_{ij}$  and set  $R_k = 3$ 
17:    else
18:      Add  $k$  to  $\text{Star}_j$  and set  $R_k = 2$ 
19:       $t_{ij}^H = t_{ij}^H + 1$ 
20:  for  $k \in \text{Star}_i$  do ▷ This internal nested loop determines computational complexity
21:    for  $(l \neq i) \in \mathcal{N}_1(k)$  do
22:      if  $R_l = 2$  then
23:         $Q_{ij} = Q_{ij} + 1$ 
24:  for  $k \in \text{Star}_i$  do
25:    Set  $q_{ij}^W = q_{ij}^W + D_k - 1$  and  $R_k = 0$ 
26:  for  $k \in \text{Star}_j$  do
27:    Set  $q_{ij}^H = q_{ij}^H + D_k - 1$  and  $R_k = 0$ 
28:  for  $k \in \text{Tri}_{ij}$  do
29:    Set  $q_{ij}^W = q_{ij}^W + D_k - 2$ 
30:    Set  $q_{ij}^H = q_{ij}^H + D_k - 2$ 
31:    Set  $R_k = 0$ 
32:  Set  $C_u = (T_{ij}, t_{ij}^W, t_{ij}^H, Q_{ij}, q_{ij}^W, q_{ij}^H)$  ▷ Set  $u$ -th row of  $C$ 
33: return  $C$ 

```

S3.2. Calculating counts for reversed edges

Note that in our implementation t_{ij}^W counts the number of (k, i, j) and t_{ij}^H tracks (i, j, k) triples. Thus, we have that $t_{ij}^W = t_{ji}^H$. Similarly, q_{ij}^W counts (j, i, k, l) and q_{ij}^H (i, j, k, l) quadruples, so again we have that $q_{ij}^W = q_{ji}^H$. On the other hand, counts of triangles and quadrangles are symmetric. As a result, for the purpose of counting we can

Table S1. Notation summary and formulas for aggregating from edge to node and global counts

	Edge	Counting level	
		Node	Global
Paths			
Wedge triples	t_{ij}^W	$t_i^W = \sum_j t_{ij}^W$	$t^W = \frac{1}{2} \sum_{i,j} t_{ij}^W$
Head triples	t_{ij}^H	$t_i^H = \sum_j t_{ij}^H$	$t^H = \frac{1}{2} \sum_{i,j} t_{ij}^H$
Wedge quadruples	q_{ij}^W	$q_i^W = \sum_j q_{ij}^W$	$q^W = \frac{1}{2} \sum_{i,j} q_{ij}^W$
Head quadruples	q_{ij}^H	$q_i^H = \sum_j q_{ij}^H$	$q^H = \frac{1}{2} \sum_{i,j} q_{ij}^H$
Cycles			
Triangles	T_{ij}	$T_i = \frac{1}{2} \sum_j T_{ij}$	$T = \frac{1}{6} \sum_{i,j} T_{ij}$
Quadrangles	Q_{ij}	$Q_i = \frac{1}{2} \sum_j Q_{ij}$	$Q = \frac{1}{8} \sum_{i,j} Q_{ij}$
Structural coefficient	(clustering, closure)		
Similarity	s_{ij}	s_i	s
Complementarity	c_{ij}	c_i	c

Table S2. Formulas for structural coefficients based on path and cycle counts

Level	Coefficient	Relational principle	
		Similarity	Complementarity
Edges	Structural	$s_{ij} = \frac{2T_{ij}}{t_{ij}^W + t_{ij}^H}$	$c_{ij} = \frac{2Q_{ij}}{q_{ij}^W + q_{ij}^H}$
Nodes	Structural	$s_i = \frac{4T_i}{t_i^W + t_i^H}$	$c_i = \frac{4Q_i}{q_i^W + q_i^H}$
	Clustering	$s_i^W = \frac{2T_i}{t_i^W}$	$c_i^W = \frac{2Q_i}{q_i^W}$
	Closure	$s_i^H = \frac{2T_i}{t_i^H}$	$c_i^H = \frac{2Q_i}{q_i^H}$
Global ¹	Structural	$s = \frac{6T}{t^W + t^H}$	$c = \frac{8Q}{q^W + q^H}$
	Clustering	$s^W = \frac{3T}{t^W}$	$c^W = \frac{4Q}{q^W}$
	Closure	$s^H = \frac{3T}{t^H}$	$c^H = \frac{4Q}{q^H}$

¹ – All global measures are equivalent.

assume that all edges are of the form $i < j$ and still be able to count everything correctly. In other words there is no need to consider each undirected edge twice.

S3.3. Computational complexity

It is clear from the structure of the three nested loops that the asymptotic worst-case computational complexity of both algorithms is $O(m\Delta S d_{\max})$ where m is the number of edges, ΔS is the maximum size of the Star_i set (see Algorithm S1) and d_{\max} is the maximum node degree. This agrees with the analysis presented by the authors of

the more general graphlet counting method [1], which inspired our **PathCensus** algorithm. However, in practice the runtime can be reduced by enforcing that edges are defined to satisfy the condition $d_i \leq d_j$ (note that this can always be done without loss of generality). The impact of this optimization can be quite significant for networks with highly heterogeneous degree distributions. For instance, in the case of the PGP web of trust network [54] ($n = 39796$, $\langle d_i \rangle = 9.91$, $d_{\max} = 1696$) it yields almost 4 times shorter runtime on average.

S4. Undirected Binary Configuration Model

We used Undirected Binary Configuration Model (UBCM) [65] for the calibration and assessment of statistical significance of structural coefficients. UBCM is a variant of the configuration model that induces a maximum entropy probability distribution over undirected and unweighted networks with n nodes constrained to have a specific expected degree sequence.

UBCM belongs to a family of Exponential Random Graph Models (ERGM) [59] which induce maximum entropy distributions over networks satisfying some constraints in expectation. Crucially, it means that such models are fully specified by a set of sufficient statistics [39] describing the desired constraints. Hence, the maximum entropy distributions they induce are maximally unbiased with respect to any other property [59].

S5. Calibrating values of structural coefficients

In the analyses comparing different networks we calibrated observed values of structural coefficients against UBCM in order to account for effects induced purely by the first-order structure (i.e. degree sequences). Such a calibration may be implemented in many different ways, but all reasonable approaches should yield qualitatively comparable results. We explain our method using an example of a calibration of a graph-level statistic such as average node-wise similarity coefficient, $\langle s_i \rangle$.

First, for an observed network G calculate the value of a graph statistic of interest, $x(G)$. Then, sample R randomized replicates G_i 's of the observed network from a chosen null model (e.g. UBCM) and calculate $x(G_i)$ for $i = 1, \dots, R$. Finally, the calibrated value of $x(G)$ based on R samples from the null model is defined as the average log-ratio of the observed value and the randomized values:

$$\mathcal{C}(x, R)(G) = \frac{1}{R} \sum_{i=1}^R \log \frac{x(G)}{x(G_i)} \quad (\text{S19})$$

S6. Assessing significance of structural coefficients

Statistical significance of node-wise structural coefficients was estimated using simulated null distributions based on R samples from UBCM. We used the fact that UBCM is a variant of the class of ERGMs [65] and therefore the probability distribution it induces is fully determined by a set of sufficient statistics [39], that is, the expected degree sequence in our case. This implies that null distributions of any statistics for nodes with the same degrees are identical, so such nodes are indistinguishable from the vantage point of the model. Thus, we estimated p -values according to the following procedure:

1. Sample R randomized analogues of an observed network G from the probability distribution induced by UBCM.
2. For each graph G_i with $i = 1, \dots, R$ calculate a vector of node-wise statistics such as structural similarity coefficient s_i .
3. Group calculated values in buckets defined by unique values of node degrees in the observed network G . Nodes in randomized networks are treated as if they had the same degrees as their corresponding nodes in G .
4. Calculate quantiles of the distributions in the buckets.
5. Set p -value for each node to $p = (1 - \alpha_{\max})$, where α_{\max} is the maximum quantile lower than the observed value for a given node. In all cases we used one hundred quantiles or percentiles.

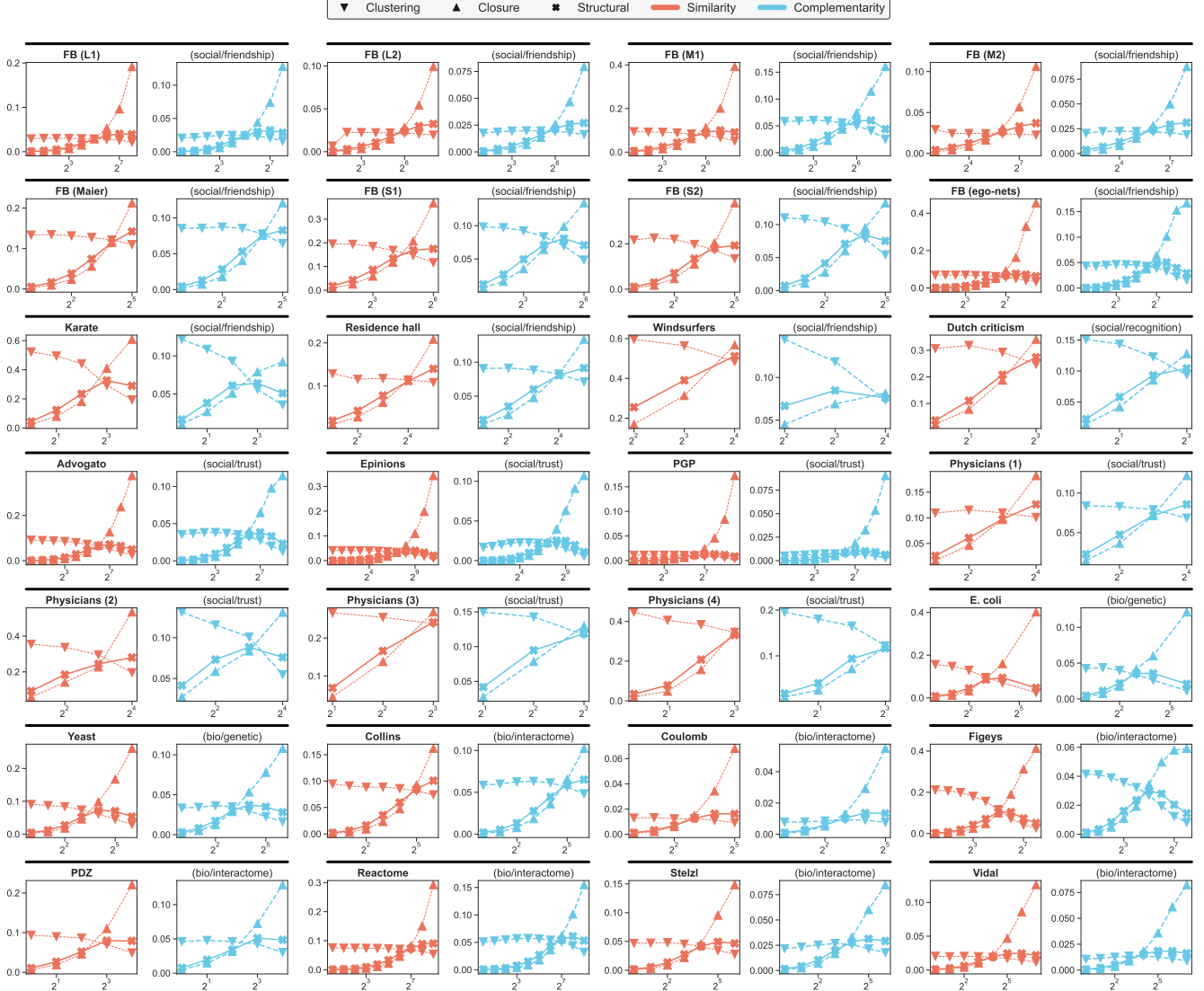


Figure S1. Correlations of clustering, closure and structural coefficients with node degrees in configuration model ensembles based on degree sequences from 28 real-world social and biological networks (see Section: Network datasets). Null distributions of the coefficients were approximated based on 100 samples from Undirected Binary Configuration Model (UBCM). The plots show values averaged for different node degrees in logarithmic bins (base 2). As evident in the figure, structural (similarity and complementarity) coefficients are always bounded between their corresponding clustering and closure coefficients. Furthermore, in all networks clustering coefficients tend to decrease for high degree nodes while closure coefficients grow with respect to degree. Thus, the analysis confirms our theoretical expectations discussed in the Main Text. Importantly, it also seems that structural coefficients in the configuration model tend to follow closure coefficients for low-degree nodes and clusterings for high-degree nodes. This suggests that the partial coefficients are good descriptors of structural similarity and complementarity only for particular parts of the degree spectrum while s_i and c_i are universally valid.

6. Adjust p -values for multiple testing using two-stage False Discovery Rate (FDR) correction proposed by Benjamini, Krieger and Yekutieli (Definition 6 in Ref. [8]).

Note that the above procedure ensures at least R observations for each node (and more for those with non-unique degrees) and therefore allows estimation of p -values with a resolution of 0.01 or better when $R \geq 100$.

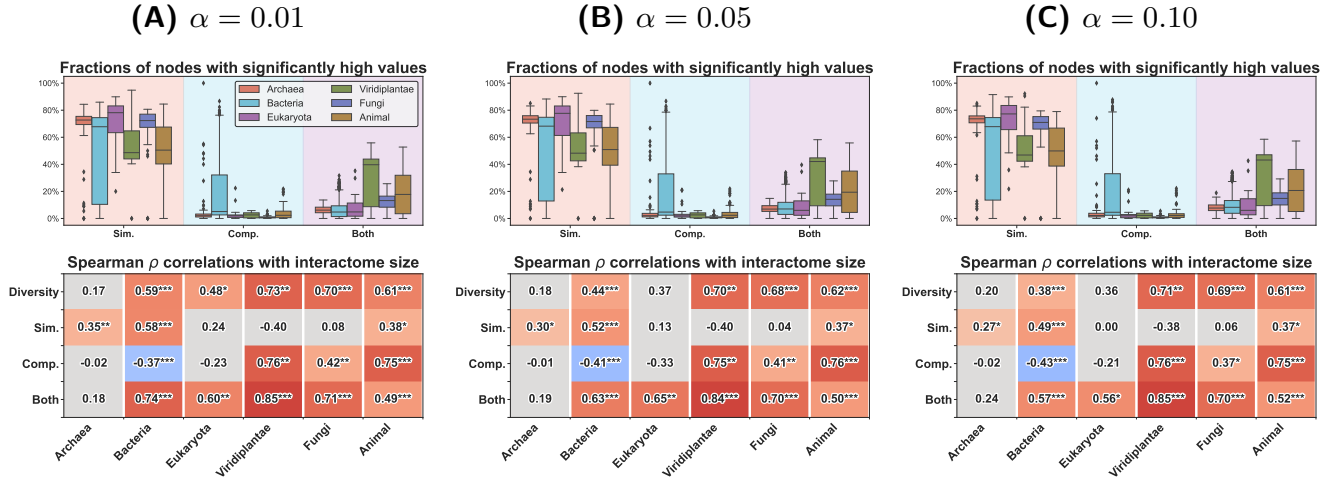


Figure S2. General characteristic of the structure of interactomes in different domains/groups. Apart from some minor details the results for all values of α are the same.

S7. Structural diversity analysis

Here we provide additional details for the corresponding analysis in the Main Text (Section: Structural diversity across the tree of life). We present results for three different choices of significance level, $\alpha = 0.01, 0.05, 0.10$ used for detecting nodes with high structural similarity and complementarity. We show that qualitative results are stable for all values of α , even though quantitative details change in some cases.

S7.1. Linear model stability and diagnostics

We described the relationship between structural diversity, $y = \mathcal{S}_\alpha(G)$, defined in Eq. [11] in the Main Text, and interactome size n (number of proteins) using a transformed linear model of the form:

$$\eta(\hat{y}) = c + \gamma \log n \quad (\text{S20})$$

where $\eta(x) = x/(1-x)$ is the logit transformation. This parametric form ensured model predictions bounded in $(0, 1)$, which was necessary as the structural diversity index ranges from 0 to 1. On the other hand, since the logit transformation is not defined for 0's and 1's we had to drop some part of the observations, namely, 119, 94 and 88 cases for $\alpha = 0.01, 0.05, 0.10$ respectively. These observations corresponded almost exclusively to organisms with small interactomes as indicated by small average numbers of nodes (35.07, 30.98 and 28.15) as compared to the overall average of 544.06 nodes. Moreover, all of them were dropped because of $\mathcal{S}_\alpha(G) = 0$, which is consistent with the hypothesis that less complex organisms tend to have less structurally diverse interactomes.

As evident in Fig. S3 the qualitative trend is the same for all values of α . However, the goodness-of-fit of the model is highest for $\alpha = 0.01$. This is not surprising. Higher values of α correspond to higher type I error rate, meaning that the estimated fractions of nodes with significantly high values of s_i and c_i are more noisy. Table S3 presents estimated parameters and other numerical details.

Moreover, since the accuracy of interactome networks may depend on the extent to which a given species has been studied, we also fitted extended models including the logarithm of the number of publications about a given species as the second predictor. This allowed controlling for effects specific only for better studied organisms. As Table S3 shows, the effects of publication count (b) were insignificant in all cases.

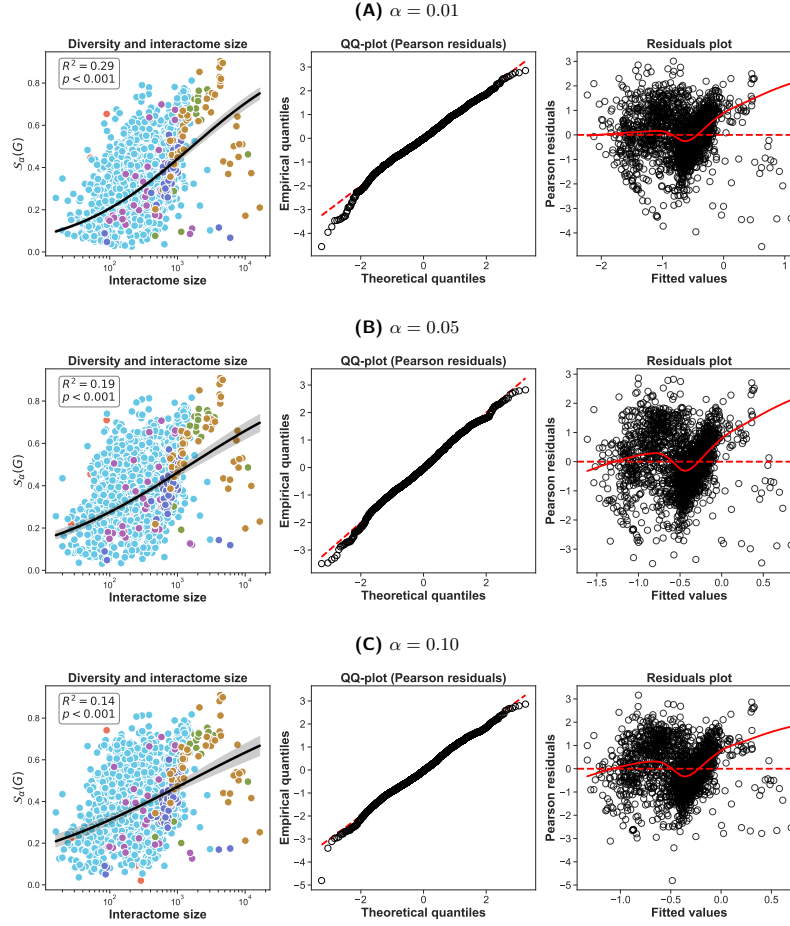


Figure S3. Model fit and residual diagnostics for $\alpha = 0.01, 0.05, 0.10$. In all cases the qualitative trend is similar but R^2 drops for higher values of α . Moreover, in all cases residuals are approximately normal apart from larger fluctuations in the region of high fitted values. This is an effect of the apparent bifurcation of the conditional distribution of the structural diversity index for species with large interactomes discussed in the Main Text.

Table S3. Estimated parameters of the linear models¹

	$\alpha = 0.01$ ($N = 1721$)				$\alpha = 0.05$ ($N = 1746$)				$\alpha = 0.10$ ($N = 1752$)			
	Value	SE	z	p	Value	SE	z	p	Value	SE	z	p
c	-3.562	0.075	-47.476	0.001	-2.595	0.133	-19.477	0.001	-2.139	0.164	-13.048	0.001
γ	0.481	0.015	32.256	0.001	0.353	0.023	15.299	0.001	0.292	0.027	10.817	0.001
	$R^2 = 0.290$, $F(1719,1) = 1040$, $p < 0.001$ Skew = -0.296, Kurtosis = 3.728 (residuals)				$R^2 = 0.188$, $F(1744,1) = 234$, $p < 0.001$ Skew = -0.134, Kurtosis = 3.135 (residuals)				$R^2 = 0.290$, $F(1750,1) = 117$, $p < 0.001$ Skew = -0.129, Kurtosis = 3.234 (residuals)			
	Models accounting for publication count (b)											
	$\alpha = 0.01$ ($N = 1662$)				$\alpha = 0.05$ ($N = 1685$)				$\alpha = 0.10$ ($N = 1752$)			
	Value	SE	z	p	Value	SE	z	p	Value	SE	z	p
c	-3.563	0.079	-44.918	0.001	-2.591	0.143	-18.175	0.001	-2.129	0.172	-12.369	0.001
γ	0.481	0.017	28.633	0.001	0.353	0.026	13.730	0.001	0.290	0.029	9.971	0.001
b	-0.0003	0.011	-0.026	0.979	0.0014	0.009	-0.155	0.876	0.0005	0.009	0.062	0.951

¹ – All global measures are equivalent.

S8. Network datasets

All network datasets were downloaded from the Netzschleuder repository [52]. In all analyses only largest connected components were used and networks were simplified by removing multilinks and self-loops. Moreover, in the case of directed or weighted networks edge directions and weights were ignored.

Individual network datasets are described below and their unique names within the repository are provided in the following subsection headings. Each dataset can be accessed via a generic link of the form: `networks.skewed.de/net/<name>` where `<name>` is a placeholder which should be substituted with the name of a specific dataset.

Below we list datasets in groups corresponding to the three empirical analyses presented in the main text. Each section ends with a table with most important descriptive statistics for all networks. The statistics were calculated for the largest connected component.

S8.1. Networks used in “*Structural coefficients in real networks*”

- **Within-organization Facebook friendships** (`facebook_organizations`)

Six undirected and unweighted networks of friendships among users on Facebook who indicated employment at one of the target corporation (S1, S2, M1, M2, L1, L2) [24]. Companies range in size from small to large. Only edges between employees at the same company are included in a given snapshot.

- **Maier Facebook friends** (`facebook_friends`)

A small anonymized Facebook ego network (undirected and unweighted), from April 2014 [40]. Nodes are Facebook profiles, and an edge exists if the two profiles are “friends” on Facebook.

- **Facebook ego-network** (`ego_social`)

The network is a combination of 10 ego-nets sampled from Facebook [45]. The network is undirected and unweighted.

- **Zachary Karate Club** (`karate`)

Undirected and unweighted network of friendships among members of a university karate club [72]. We used the corrected version with 78 instead of 77 edges.

- **ANU Residence Hall network** (`residence_hall`)

A network of friendships among students living in a residence hall at Australian National University [26]. The original network is directed and weighted with edges indicating that resident i named resident j as a friend, and weight indicating the level of friendship: 5 (best friend), 4 (close friend), 3 (friend), 2, 1.

- **Windsurfers network** (`windsurfers`)

A network of interpersonal contacts among windsurfers in southern California during the Fall of 1986 [25]. The original network is weighted with weights indicating the perception of social affiliations majored by the tasks in which each individual was asked to sort cards with other surfer’s name in the order of closeness.

- **Dutch literary criticism** (`dutch_criticism`)

A network of criticisms among Dutch literary authors in 1976 [20]. The directed edge (i, j) denotes that an author i passed judgment on author j ’s work in an interview or review. The original network is also signed and have positive and negative edges (representing positive and negative judgements). The edge signs were ignored in our analyses.

- **Advogato trust network** (`advogato`)

A network of trust relationships among users on Advogato, an online community of open source software developers [43]. Edge direction indicates that node i trusts node j , and edge weight denotes one of four increasing levels of declared trust from i to j : observer (0.4), apprentice (0.6), journeyer (0.8), and master (1.0).

- **Epinions trust network** (`epinions_trust`)

A who-trusts-whom social network of the general consumer review site *Epinions.com* [53]. Members can decide whether to “trust” each other. These trust relationships are combined with review ratings to determine which reviews are shown to the user.

- **PGP web of trust** (`pgp-strong`)

Strongly connected component of the Pretty-Good-Privacy (PGP) web of trust among users, circa November 2009 [54].

- **Physician trust network** (`physician_trust`)

A network of trust relationships among physicians in four midwestern (USA) cities in 1966 [17]. Edge direction indicates that node i trusts or asks for advice from node j . Each of the four components represent the network within a given city. We analyzed four (disconnected) components corresponding to different cities as separate networks.

- **E. coli transcription network** (`ecoli_transcription`)

Directed network of operons and their pairwise interactions, via transcription factor-based regulation, within the bacteria *Escherichia coli* [58]. In our analyses we used v1.1 version and did not distinguish between different regulation types.

- **Yeast transcription network** (`yeast_transcription`)

Directed network of operons and their pairwise interactions, via transcription factor-based regulation, within the yeast *Saccharomyces cerevisiae* [48]. We did not distinguish between different regulation types.

- **Collins yeast interactome** (`collins-yeast`)

Undirected and unweighted network of protein-protein interactions in *Saccharomyces cerevisiae* (budding yeast), measured by co-complex associations identified by high-throughput affinity purification and mass spectrometry (AP/MS) [18].

- **Coulomb yeast interactome** (`interactome-yeast`)

An undirected and unweighted network of protein-protein binding interactions among yeast proteins [19]. Nodes represent proteins found in yeast (*Saccharomyces cerevisiae*) and an edge represents a binding interaction between two proteins.

- **Figeys human interactome** (`interactome_figeys`)

A directed unweighted network of human proteins and their binding interactions [23]. Nodes represent proteins and an edge represents an interaction between two proteins, as inferred using a mass spectrometry-based approach.

- **PDZ-domain interactome** (`interactome_pdz`)

An undirected and unweighted network of PDZ-domain-mediated protein-protein binding interactions, extracted from the PDZBase database [9]. Nodes represent proteins and an edge represents a binding interaction between two proteins.

- **Joshi-Tope human protein interactome** (`reactome`)

An undirected and unweighted network of human proteins and their binding interactions, extracted from Reactome project [32]. Nodes represent proteins and an edge represents a binding interaction between two proteins.

- **Stelzl human interactome** (`interactome_stelzl`)

A directed unweighted network of human proteins and their binding interactions [61]. Nodes represent proteins and an edge represents an interaction between two proteins, as inferred via high-throughput Y2H experiments using bait and prey methodology.

- **Vidal human interactome** (`interactome_vidal`)

An undirected and unweighted network of human proteins and their binding interactions [56]. Nodes represent proteins and an edge represents a binding interaction between two proteins, as tested using a high-throughput yeast two-hybrid (Y2H) system.

Table S4. Descriptive statistics ($N = 28$)

domain	dataset	network	s	c	n	S	ρ	$\langle d_i \rangle$	σ_{d_i}	d_{\max}
biological	collins_yeast	v1.1	0.62	0.01	1004	0.62	0.02	16.57	1.12	127
	ecoli_transcription		0.02	0.05	328	0.78	0.01	2.78	1.86	72
	interactome_figey		0.01	0.14	2217	0.99	0.00	5.79	2.95	314
	interactome_pdz		0.00	0.21	161	0.76	0.02	2.60	1.12	21
	interactome_stelzl		0.01	0.12	1615	0.95	0.00	3.85	1.85	95
	interactome_vidal		0.04	0.03	2783	0.89	0.00	4.32	1.63	129
	interactome_yeast		0.05	0.01	1458	0.78	0.00	2.67	1.29	56
	reactome		0.61	0.05	5973	0.94	0.01	48.81	1.39	855
social	yeast_transcription	facebook_combined	0.02	0.19	664	0.72	0.00	3.21	1.79	71
	advogato		0.09	0.02	5042	0.77	0.00	15.56	2.07	803
	dutch_criticism		0.16	0.22	35	1.00	0.13	4.57	0.65	12
	ego_social		0.52	0.02	4039	1.00	0.01	43.69	1.20	1045
	epinions_trust		0.07	0.02	75877	1.00	0.00	10.69	4.02	3044
	facebook_friends		0.51	0.02	329	0.91	0.04	11.88	0.92	63
	facebook_organizations	L1	0.26	0.04	5793	1.00	0.00	10.62	1.73	320
		L2	0.22	0.02	5524	1.00	0.01	34.11	0.93	417
		M1	0.26	0.03	1429	1.00	0.02	27.09	1.06	339
		M2	0.23	0.02	3862	1.00	0.01	45.22	0.65	328
		S1	0.29	0.03	320	1.00	0.05	14.81	0.96	113
		S2	0.33	0.03	165	1.00	0.05	8.80	0.95	63
	karate	78	0.26	0.06	34	1.00	0.14	4.59	0.83	17
	pgp_strong	1	0.25	0.01	39796	1.00	0.00	9.91	2.46	1696
	physician_trust	2	0.17	0.05	117	1.00	0.07	7.95	0.50	26
		3	0.28	0.06	48	1.00	0.16	7.46	0.62	28
		4	0.32	0.08	41	1.00	0.17	6.93	0.42	15
		4	0.42	0.07	35	1.00	0.23	7.83	0.48	15
	residence_hall		0.30	0.04	217	1.00	0.08	16.95	0.46	56
	windsurfers		0.56	0.03	43	1.00	0.37	15.63	0.42	31

s - global similarity (clustering)

c - global complementarity

n - number of nodes in the giant component

S - relative size of the giant component

ρ - edge density

$\langle d_i \rangle$ - average node degree

σ_{d_i} - coefficient of variation of node degrees

d_{\max} - maximum node degree

S8.2. Networks used in “*Similarity and complementarity in social relations*”

- **Ugandan village networks (ugandan_village)**

The dataset consists of unweighted and undirected networks of friendship and health advice relations between households in 17 rural villages bordering Lake Victoria in Mayuge District, Uganda. It has been originally studied in Ref. [15]. Relations were measured using the name generator approach in which a representative of each household was asked to indicate up to 10 persons considered friends or trustworthy in regard to health issues. Resulting ties were symmetrized.

Table S5. Descriptive statistics ($N = 34$)

domain	dataset	network	s	c	n	S	ρ	$\langle d_i \rangle$	σ_{d_i}	d_{\max}
social	ugandan_village	friendship-1	0.06	0.03	202	1.00	0.03	5.42	0.72	32
		friendship-2	0.11	0.05	181	0.99	0.04	7.60	0.77	44
		friendship-3	0.13	0.06	192	1.00	0.06	11.04	0.74	53
		friendship-4	0.09	0.05	320	1.00	0.04	12.97	0.66	50
		friendship-5	0.12	0.05	184	1.00	0.04	7.83	0.69	30
		friendship-6	0.14	0.07	139	1.00	0.07	9.09	0.68	42
		friendship-7	0.17	0.09	121	1.00	0.11	12.73	0.52	32
		friendship-8	0.06	0.04	369	1.00	0.03	9.50	0.70	58
		friendship-9	0.16	0.06	178	1.00	0.07	12.02	0.78	80
		friendship-10	0.10	0.07	207	1.00	0.05	10.55	0.64	44
		friendship-11	0.09	0.04	250	1.00	0.03	8.50	0.70	44
		friendship-12	0.08	0.05	229	1.00	0.03	7.62	0.86	58
		friendship-13	0.10	0.06	183	1.00	0.05	8.84	0.68	34
		friendship-14	0.15	0.06	124	1.00	0.07	8.47	0.64	36
		friendship-15	0.07	0.04	120	1.00	0.04	4.57	0.70	17
		friendship-16	0.05	0.03	372	1.00	0.02	7.38	0.72	43
		friendship-17	0.25	0.07	65	1.00	0.12	7.91	0.70	31
		health-advice_1	0.05	0.04	187	0.98	0.02	4.61	1.31	60
		health-advice_2	0.06	0.06	170	1.00	0.03	4.64	1.66	70
		health-advice_3	0.08	0.05	185	1.00	0.04	6.90	1.43	78
		health-advice_4	0.06	0.04	316	1.00	0.02	6.61	0.96	72
		health-advice_5	0.09	0.02	166	0.99	0.03	4.65	1.45	70
		health-advice_6	0.06	0.02	131	0.98	0.03	4.34	1.93	75
		health-advice_7	0.14	0.06	121	1.00	0.07	7.82	0.80	46
		health-advice_8	0.05	0.03	361	1.00	0.02	6.85	1.04	84
		health-advice_9	0.10	0.05	173	1.00	0.04	7.20	1.42	98
		health-advice_10	0.13	0.05	204	1.00	0.04	8.04	0.98	71
		health-advice_11	0.05	0.04	234	0.97	0.02	4.50	1.67	85
		health-advice_12	0.04	0.04	218	0.99	0.02	4.90	1.30	79
		health-advice_13	0.06	0.03	157	0.91	0.02	3.64	1.25	51
		health-advice_14	0.11	0.05	120	1.00	0.05	5.43	0.80	26
		health-advice_15	0.06	0.05	117	1.00	0.03	3.35	1.36	34
		health-advice_16	0.04	0.01	349	1.00	0.01	4.94	2.21	152
		health-advice_17	0.13	0.06	63	1.00	0.07	4.63	0.95	28
Average			0.09	0.05	197.29	0.99	0.04	7.21	1.01	56.09

s - global similarity (clustering)

c - global complementarity

n - number of nodes in the giant component

S - relative size of the giant component

ρ - edge density

$\langle d_i \rangle$ - average node degree

σ_{d_i} - coefficient of variation of node degrees

d_{\max} - maximum node degree

S8.3. Networks used in “*Structural diversity across the tree of life*”

For this analysis we used a dataset of 1840 interactomes of different species across the tree of life published originally in Ref. [74]. The interactomes represent only physical protein-protein interactions that are experimentally supported or manually curated. Detailed description of the dataset and its underlying methodology, including the list of types of interactions that were considered, can be found in the Supplementary Information appendix of Ref. [74]. In particular, information on phylogenetic taxonomy information, the source of publication counts per species and evolution time estimates are discussed in sections S1.2, S2.2 and S3.

Due to the large number of networks we do not present a table with descriptive statistics here. The data and code used for conducting the analysis is available from the Github repository listed in the Main Text (Data and materials availability).

S9. Experimental assessment of the performance of PathCensus algorithm

We assessed the performance of our implementation of **PathCensus** algorithm by measuring the average runtime for each of the 1840 interactome networks studied in the paper as well as their randomized counterparts sampled from UBCM. For each network an average runtime over 5 runs was calculated for the observed network and a corresponding randomized version sampled from UBCM (see Fig. S4).

Our analysis shows that the runtime scales approximately linearly with respect to $|E|\Delta Sd_{\max}$, which agrees with the previous theoretical analysis of the computational complexity of **PathCensus** algorithm. However, the proportionality constant is lower for smaller networks and then increases for networks with about 100 nodes. After that, the linear scaling seems to be stable.

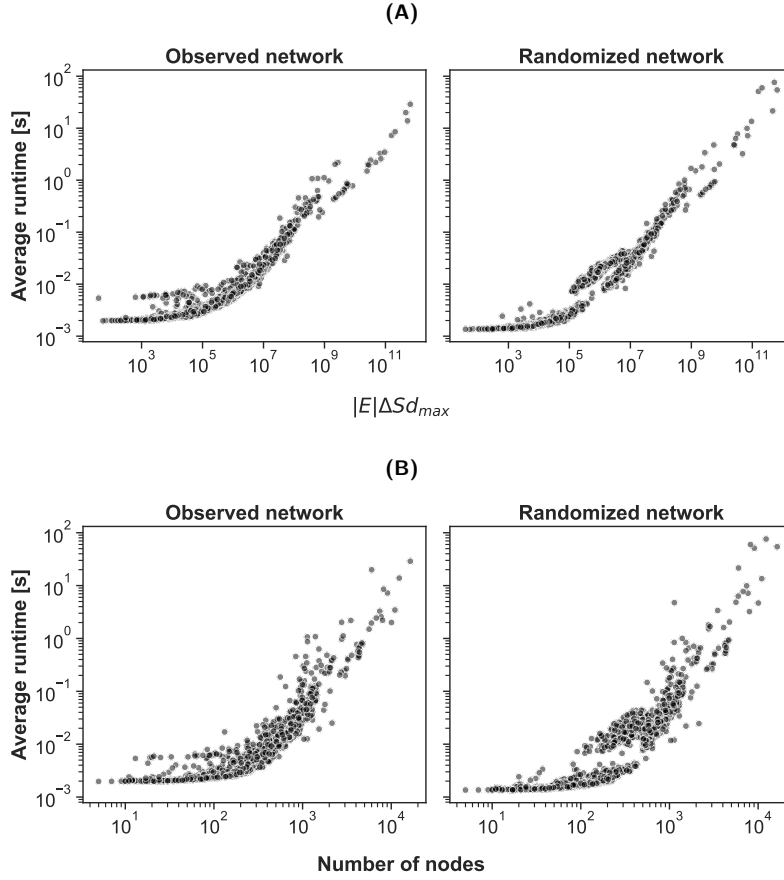


Figure S4. Experimental assessment of the performance of PathCensus algorithm. Computations used the $d_i \leq d_j$ optimization discussed in Algorithm S1. **(A)** Average runtime plotted against the product of the number of edges ($|E|$), maximum node degree (d_{\max}) and the maximum size of a Star_i set (ΔS ; see Algorithm S1). **(B)** Average runtime and network size.